Title

AN INVESTIGATION OF THE INFLUENCE OF DISLOCATION SUBSTRUCTURES ON THE DEFORMATION BEHAVIOR OF AK, DQ STEEL SHEETS

Author

Vincent, S.A.

Publication Date

1987-12-01

Center for Advanced Materials

CAM

An Investigation of the Influence of Dislocation Substructures on the Deformation Behavior of AK, DQ Steel Sheets

S.A. Vincent
(M.S. Thesis)

December 1987

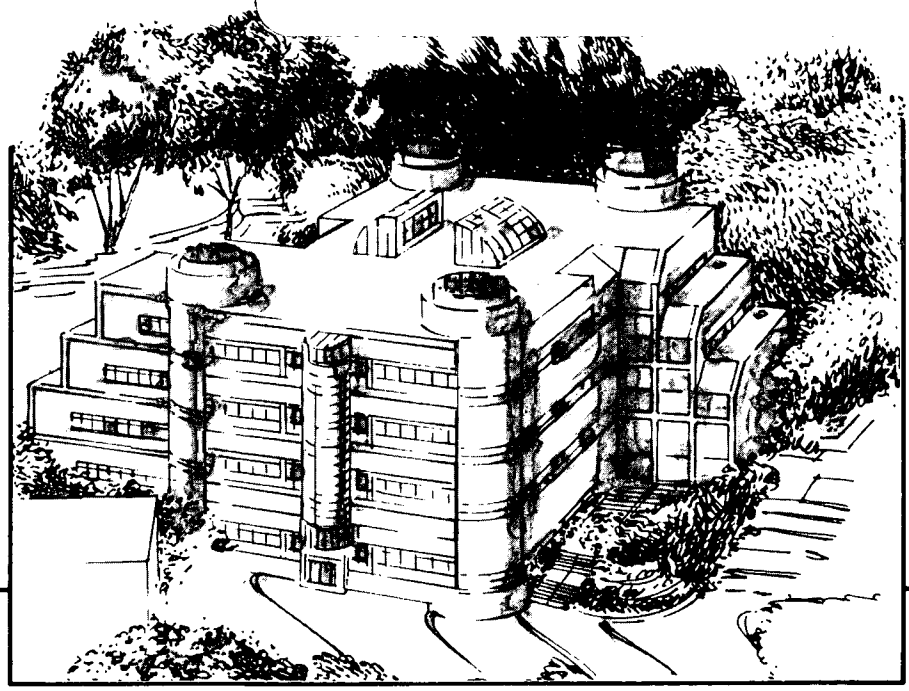

Materials and Chemical Sciences Division

Lawrence Berkeley Laboratory • University of California

ONE CYCLOTRON ROAD, BERKELEY, CA 94720 • (415) 486-4755

Prepared for the U.S. Department of Energy under Contract DE-AC03-76SF00098

DISCLAIMER

LBL-24443

AN INVESTIGATION OF THE INFLUENCE OF DISLOCATION SUBSTRUCTURES ON THE DEFORMATION BEHAVIOR OF AK, DQ STEEL SHEETS

SUE A. VINCENT
M.S. THESIS

Department of Materials Science and Mineral Engineering
University of California at Berkeley

and

Center for Advanced Materials
Materials and Chemical Sciences Division
Lawrence Berkeley Laboratory
University of California
Berkeley, California 94720

December 1987

This work is supported by the Director, Office of Energy Research, Office of Basic Energy Science, Material Sciences Division of the U.S. Department of Energy under control No. DE-AC03-76SF00098

Acknowledgements

I would like to express my appreciation to many people for their assistance in this endeavor. My gratitude is extended to Professor J. W. Morris, Jr., for his support; to my thesis committee, Professors George Johnson and Tom Devine, for their review of my thesis; to Dr. Robin Stevenson of General Motors Corporation for his support and valuable suggestions; and to Dr. Mike Stout of Los Alamos National Laboratory for his encouragement and many helpful discussions.

Virtually every member of Prof. Morris' research group has helped me at one time or another, and I would like to extend my thanks to all for their assistance. Special thanks go to Dr. Kotobu Nagai, Roger Emigh, and David Chu for help with the tensile experiments and data processing; to Yoonsoon Im and Steve Shaffer for assistance with the TEM work; to Mei Zequn for his review of my thesis; to Jin Chan for experimental assistance and several helpful suggestions; and to Judy Glazer for many interesting and valuable discussions, and for her review of this thesis.

My deepest gratitude is extended to my husband, Charlie, for his patience and continuous support. Thanks also go to my parents, John and Phyllis Alexander, and to my brother, James Alexander, for their encouragement.

This work was supported by the Director, Office of Energy Research, Office of Basic Energy Science, Material Sciences Division of the U.S. Department of Energy under control No. DE-AC03-76SF00098. Financial support for this work was also provided by General Motors Corporation.

Contents

1. Introduction

Automobiles, airplanes, Bar-B-Que grills, and golf clubs -- many of the things held dear by people today contain parts made by some type of forming process. The manufacturers of these products are often required to challenge the formability of these various components. "Can this sheet be made thinner to save weight and increase fuel economy?" "Can we use stiffer or stronger material for this part, and still be able to form it to the shape we need?" What can be done to better understand, and hopefully improve, metal formability?

This research was undertaken as part of an effort sponsored by General Motors Corporation to improve sheet metal formability through a better understanding of the material's role in the process. Previous work by this group in this area has included investigations from two different approaches. The first study (Shaffer, 1986) examined the effect of material cleanliness, or inclusion content, on its formability. Shaffer found that at the present low levels of inclusion content, this factor is not playing an important role. The second study (Ledezma, 1986) was a more fundamental look at the deformation process itself. Using transmission electron microscopy (TEM), Ledezma characterized the three-dimensional dislocation substructure that forms in low carbon steel sheet during punch stretching. She found that, at least in the case of biaxial stretching (positive minor strain), the orientations of the dislocation cell walls are related to the predicted active slip planes. This conclusion was the springboard for this study. The intriguing question was this: since the substructure seems to be related to deformation geometry, what role does its formation and presence play in the deformation process?

The material studied in the aforementioned works was aluminum-killed drawing quality (AK DQ) low carbon steel sheet of the type used for automotive skin panels. That material choice proved to be a good one for this study; dislocation strengthening effects

can be studied experimentally in this material since the primary hardening mechanism is dislocation strengthening.

To compare the effects of substructure, or dislocation arrangement patterns, on deformation, one must have more than one type of substructure for comparison, while holding other variables as constant as possible. As described more fully in the Background section of this thesis, the type of substructure that forms depends primarily on how easily dislocations can cross-slip in the material. Since cross-slip is relatively easy in body-centered cubic steel under normal conditions, a three-dimensional cellular-type structure commonly forms. In order to form a different substructure, particularly a non-cellular structure, cross-slip must somehow be inhibited.

The work of Keh and Weissmann (1963) provided a solution to this dilemma. Keh and Weissmann's work on pure iron indicated that if the material was deformed at a sufficiently low temperature to inhibit cross-slip, a non-cellular type structure formed, even at moderate strains. Thus it seemed that it should be possible to develop deformed specimens with different substructures and compare their subsequent deformation behavior to try to determine what effect the substructure has on deformation behavior.

To summarize, the purpose of this study was to observe the effect of dislocation substructure on the deformation behavior of low carbon steel sheet, and to search this information for clues about the effects of these substructures on work hardening behavior. The method included first developing different types of substructures in otherwise identical specimens by prestraining at different temperatures. These specimens were then subjected to continued deformation at the same temperature. The tensile behavior was then analyzed, bearing in mind the substructural changes, in an effort to improve the fundamental understanding of the deformation process.

2. Background

2.1 Dislocation Substructure

2.11 Definition of Dislocation Substructure

The term "dislocation substructure" refers to the arrangement of dislocations within the grains of a material, especially after it has been deformed. For the purposes of this study there are basically two types of substructures: cellular and non-cellular. In a cellular substructure the dislocations are gathered into high density "cell walls" which surround regions that are relatively free of dislocations. These cell walls are similar to very low angle grain boundaries. The orientation difference across the walls depends on the density of dislocations in the walls and is greater as the amount of deformation increases and more dislocations become part of the walls. Non-cellular substructures can take a variety of forms; however, in general they are characterized by the absence of cell walls surrounding areas of low dislocation density. The dislocations are sometimes randomly distributed throughout the grains, sometimes gathered in clusters, or sometimes aligned parallel within the grain.

The type of substructure that eventually evolves depends on the ability of dislocations to move readily through the material. In body-centered cubic (bcc) materials and high stacking fault energy face-centered cubic (fcc) materials, dislocations can generally cross-slip and move on more than one family of slip planes. This three-dimensional ease of movement facilitates the formation of a three-dimensional network: cell walls. Materials with these characteristics usually form a cellular-type dislocation substructure when deformed to moderate strains. On the other hand, in low stacking fault energy fcc materials or in cases where cross-slip is hampered in some way, dislocations cannot readily move in a three-dimensional way. In this case cell formation is difficult,

especially in the early stages of deformation when there are few obstacles to prevent slip on primary slip planes. The dislocations then form the non-cellular structures described above. Sometimes these materials will eventually form a cell structure after large amounts of deformation, when large pile-ups of dislocations prevent easy movement on primary slip systems.

As ferritic steels are bcc materials, the dislocation substructure that forms under normal deformation conditions is cellular. However, when the deformation occurs at a sufficiently low temperature, cross-slip becomes more difficult. Cross-slip involves a change in the path of a dislocation from one slip system, with a given critical resolved shear stress, to another system, with a critical resolved shear stress of similar magnitude. This change in slip system can be impeded due to both the difference in the critical resolved shear stresses of the two slip systems, and the reduction in the mobility of a dislocation extended over more than one slip plane. At normal temperatures cross-slip may occur despite this difficulty, especially if the resistance to slip on the initial slip system is high. When sufficient thermal energy is available, the probability that the dislocation motion on the new slip system will be activated is increased, and the dislocation will be more likely to cross-slip. At low temperatures this change in slip system is made more difficult because there is less thermal energy available to activate the process of slip system change. Under these conditions when cross-slip is difficult, one might expect to find a non-cellular type structure. As will be discussed later, this is indeed the case.

2.12 The Effect of Dislocation Substructure on Deformation Behavior: Current Theories

Current theories of work hardening have been recently reviewed by Kuhlmann-Wilsdorf (1985) and previously by Gil Sevillano et al. (Gil Sevillano, van Houtte, and Aernoudt, 1980). Virtually all of the current theories incorporate some description of

dislocation arrangements. Since dislocation motion is involved in most modes of plastic deformation, this is quite understandable. In the second review (Gil Sevillano et al.) current theories are divided into two types, depending on whether the flow stress is determined by 1.) the stress needed to activate a dislocation source ("multiplication controlled flow stress"), or 2.) the stress necessary for a dislocation to bypass an obstacle ("propagation controlled flow stress").

The multiplication-controlled models include mathematical descriptions of various types of dislocation sources. A lower bound model proposes multiplication from helical sources originating from a free dislocation segment pinned at one end to a cell or subgrain wall (Ashby, 1966; Brown and Ham, 1971). Kuhlmann-Wilsdorf's "meshlength theory" (1962, 1968, 1970, 1977) describes dislocations produced by the bending of the longest free dislocation link that is pinned at both ends by the existing substructure. Li's theory (1963a, 1963b) concerns the emission of dislocations from subgrain boundaries or sources in the vicinity of subgrain boundaries. The first and third theories describe dislocation multiplication in only certain regimes of substructure development, while the "meshlength theory" can apply to the entire range of substructures.

The propagation-controlled theories propose various ways in which dislocations or groups of dislocations inhibit the movement of gliding dislocations. Langford and Cohen (1969, 1970) assume that the cell and subgrain walls are impenetrable, and propose a lower bound for the stress needed to propagate a dislocation that is determined by the stress needed to expand a dislocation loop in the free slip area within the cell or subgrain. "Forest" dislocation theories treat the forest of dislocations that intersect the slip plane as an array of point obstacles, and calculate the stress needed to pass a dislocation by this array (there are several models of this type as reviewed by Brown and Ham, 1971). Other theories propose that the flow stress is controlled by the long range internal stresses from dislocation groups piled up at obstacles (Taylor, 1934; Seeger, 1957; Hirsch and Mitchell, 1968). Li (1963a) also proposed a model concerned with the long range stress from

subgrain boundaries, and many of the Hall-Petch type models (grain boundaries as dislocation barriers) can be included in this category (reviewed by Li and Chou, 1970). Again, some of these models ("forest" and long range stress theories) can be applied to all ranges of substructure development, while others are restricted to certain regimes.

It is interesting to note that, regardless of the diversity of assumptions and mechanisms, all of these models lead to equations of essentially the same form. This is perhaps an indication that the role of substructure in work hardening is not well understood.

Many of the current theories discuss the formation of dislocation substructure as a result of deformation. Theories such as Kuhlmann-Wilsdorf's "meshlength theory" describe the formation of dislocation substructure as a result of an applied stress. During deformation, dislocations arrange themselves into the most stable network permitted by the dislocation mobility. As deformation continues, this network is maintained, but the scale is reduced proportionately to the increase in stress. The implication here is that the dislocation substructure is a reaction of the material to the applied stress conditions: an "effect" of the deformation behavior rather than a cause.

As discussed briefly in the Introduction, Ledezma's work (1986) could perhaps suggest another conclusion, i.e. that the substructure has a more active role in determining deformation behavior. Ledezma's observation that the dislocation substructure is geometrically related to slip conditions in the material suggests that the dislocation configuration may have some bearing on the deformation process. For instance, the alignment of dislocation cell walls along active slip planes suggests that the cell structure may facilitate slip by concentrating dislocation activity along slip planes; or conversely the gathering and tangling of dislocations along the slip planes may increase the flow stress required for these dislocations to move or cause the activation of more dislocation sources.

This investigation seeks to ascertain whether the role of dislocation substructure is one of "effect" or perhaps one of "cause." Comparison of deformation behavior of materials with different substructures should shed some light on this topic.

2.2 Testing the Effect of Substructure on Deformation

2.21 Experiment Design

A set of experiments was designed based on the work of Keh and Weissmann (1963) on pure iron. Keh and Weissmann found that Fe specimens deformed above 3.5% strain at 25°C had formed the beginnings of a cell structure, and this structure was well-developed in most grains by 9% strain. In specimens deformed at -75°C a cell structure did not form below 16% strain. At even lower temperature, a specimen deformed 13% at -135°C had a substructure consisting of a generally uniform distribution of dislocations, with no cell walls present.

To study the effect of prestraining at different temperatures on the dislocation substructure formation, Keh and Weissmann prestrained specimens at one temperature, then continued the straining at another temperature. A specimen deformed 13% at -135°C followed by 19% at room temperature was found to have a well developed cell structure, as if all of the deformation had occurred at room temperature. In contrast, a specimen deformed 8% at room temperature followed by 5.5% at -135°C was found to have a cell structure with some dislocations in the interior of the cells. Apparently the cell structure that formed initially at room temperature prevailed when the straining was continued at low temperature. These observations led to the interesting question: what are the macroscopic consequences of these microscopic processes? To answer this question, experiments similar to Keh and Weissman's were performed in this study, with the mechanical behavior of the specimens during these changes as the focus.

From the starting point of Keh and Weissmann's TEM observations at these temperatures, preliminary testing was done to select a "low" temperature for AK DQ steel at which no cellular substructure formed, even at strains as large as 15%. Tensile specimens were deformed 15% at a variety of temperatures, and the dislocation substructures were characterized using TEM. In initial testing, specimens deformed in uniaxial tension at liquid nitrogen temperature (-196°C) fractured in a brittle manner, indicating that the deformation temperature must be sufficiently high to avoid ductile-to-brittle transition. Specimens deformed 15% at -100°C exhibited no brittle behavior; substructures were found to consist of random arrays of dislocations and some dislocation pile-ups, but no cell walls were present. Thus -100°C was chosen to be the "low" temperature for prestraining to form a non-cellular dislocation substructure. TEM studies of specimens deformed 15% at room temperature were found to have well-developed cellular dislocation substructures, and room temperature was therefore chosen for the prestraining temperature to form a cellular dislocation substructure.

Two criteria were used to choose the amounts of prestraining for this study. The first was to prestrain to a level sufficient to allow initial substructure development. Given Keh and Weissmann's observations (1963) that cell formation was well underway by 3.5% strain at room temperature, and our preliminary observations that the substructure was well-developed at both temperatures at 15% strain, the range of strains was narrowed to within 3.5% to 15% strain. The second criterion was to ensure that the deformation in the specimen was uniform, i.e. less than the point of diffuse necking. To satisfy this, uniaxial tensile tests were performed at room temperature and -100°C. Stress-strain curves were plotted, and the strain hardening rates (slopes of the curves) were calculated and plotted against strain. Using the criterion for diffuse necking for sheets (for a discussion of diffuse and local necking in sheets, see Backofen, 1972, for example), that is that the strain hardening rate is equal to the true stress, it was determined that diffuse necking at room temperature occurs around 23% strain and at -100°C around 13% strain. To satisfy the

above criteria prestrains of 5% and 10% at -100°C were chosen, with 5% being perhaps "early" for complete substructure development, but interesting nonetheless.

As described more thoroughly in the next section, the flow stress at room temperature (abbreviated as RTFS) was chosen as the state parameter for deformation for these experiments. Thus the prestrains at room temperature are described not in terms of strain, but in terms of the RTFS associated with 5% or 10% strain at -100°C, designated as "RTFS-5%" and "RTFS-10%", respectively.

2.22 A State Parameter to Describe "Equivalently Deformed" States

To compare materials of different substructures which have been deformed "equivalent" amounts, it is first necessary to find some parameter to describe "equivalently deformed" states. In the case of elastic deformation this problem is straightforward. As is discussed by Morris (1987), the appropriate constitutive coordinates to describe elastic deformation are the stress and strain tensor. In elasticity it is possible to define a reference state and describe an elastically deformed state as a difference between the new equilibrium state and the reference state. Unfortunately this approach is not appropriate for large scale plasticity because the reference state cannot be uniquely defined. After a material has been plastically deformed, it cannot return to its original unstrained state. Thus a different approach, one that takes into consideration the structural changes in the material, must be employed. (This subject has been discussed by several authors. The interested reader should consult Kocks, Argon and Ashby (1975) for a more in-depth discussion and reference list.)

The type of parameter needed for this study had two main qualifications: it should adequately describe the material's resistance to further deformation under some set of conditions; and it should be measurable. Follansbee (Follansbee and Kocks, 1986; Follansbee, 1986) suggested that an appropriate parameter would be the Mechanical

Threshold Stress, or the flow stress at zero Kelvin. This parameter essentially describes the stress required to overcome the maximum glide resistance of the lattice without thermal activation, and thus indicates the material's resistance to further deformation in the absence of thermal effects.

The problem with this parameter involves its measurement. The method for measuring the Mechanical Threshold Stress involves measuring the flow stress at a variety of temperatures and extrapolating to zero Kelvin. Because this method is experimentally difficult, especially in metals that undergo ductile-to-brittle transitions, an alternative was sought. Considering the nature of the parameter with respect to thermal activation, it seemed reasonable that a parameter that describes the glide resistance with some constant amount of thermal activation would be adequate. Thus the flow stress at room temperature at the same true strain rate was chosen as the state parameter. The conditions which were considered "equivalent" were:

1. 5% strain at -100°C, and the amount of deformation at room temperature required to attain the same Room Temperature Flow Stress ("RTFS-5%")
2. 10% strain at -100°C, and the amount of deformation at room temperature required to attain the same RTFS ("RTFS-10%").

3. Experimental Procedure

3.1 Tensile Testing

The following tensile tests were performed as part of this study:

1. tensile tests at room temperature and -100°C
2. 5% strain at -100°C, followed by straining to failure at room temperature
3. 10% strain at -100°C, followed by straining to failure at room temperature
4. straining to RTFS-5% at room temperature, followed by straining to failure at -100°C
5. straining to RTFS-10% at room temperature, followed by straining to failure at -100°C

3.11 Specimen Preparation

The material used in this study was aluminum killed drawing quality low carbon steel sheet of .030 inch thickness supplied by General Motors Corporation. Mechanical properties and composition data as supplied by GM are listed in Tables 1 and 2. As a normal part of processing, this material had been temper rolled less than 2% to alleviate yield point inhomogeneities in its tensile behavior.

1-1/2" X 6" sheet tensile specimen blanks were sheared from the sheet in the longitudinal direction. Stacks of approximately 15 blanks were then clamped together, and holes for pin grips were drilled. The specimens were then mounted on a custom jig, and gage sections were end-milled out to the final dimensions shown in Figure 1 (gage section dimensions 1" x 3/8"). This specimen design was chosen to allow adequate gage section material for TEM specimen preparation.

3.12 Testing Equipment

Tensile testing was performed on a custom built load frame designed and built at Lawrence Berkeley Laboratory. A compression tube - pull rod assembly was used to facilitate low temperature testing. For the low temperature tests the specimen and surrounding assembly were immersed in a -100°C mixture of isopentane and liquid nitrogen. The temperature was monitored using a low temperature thermometer and was controlled within ±3°C over the duration of the test. Referring to tests 2-5 as listed in Section 3.1, the specimens were only partially unloaded during the temperature changes. Some unloading was necessary to avoid deformation of the specimen due to differential expansion and contraction of the testing assembly; however, a small load was maintained to avoid possible relaxation of the dislocation substructure during the elapsed time.

Test control and data acquisition were achieved through an IBM AT computer attached to the load frame. The tests were run under stroke control, calibrated to maintain a constant true strain rate of 2% per minute (approximately 3×10^{-4} sec^{-1}). Constant true strain rate was used, rather than conventional constant displacement rate (which causes a declining true strain rate as the test progresses) to better isolate the behavioral differences due to temperature only. This was accomplished using an exponential wave form, rather than the conventional ramp form. Load cell sensitivity was within 1 lb. One data point, including time, load, stroke, strain, and valve current, was taken every 0.35 second. Data files for the tests were transferred to a Macintosh Plus computer using Macintosh's MacTerminal software.

3.13 Data Processing

The test data files were processed using the Fortran programs listed in Appendix 1. A brief summary of the functions of these programs is also given in Appendix 1.

3.2 TEM Confirmation of Substructures

Transmission Electron Microscopy techniques were used to determine the dislocation substructure characteristics of the specimens used in this study. A brief explanation of the pertinent techniques and conditions follows.

3.2.1 Specimen Preparation

Gage section regions of the tensile specimens of interest were chemically thinned to approximately 0.005 inch using a solution of 5% HF in H_2O_2 (30%). 3 mm discs were then punched from the sheets and carefully ground on 600 grit SiC paper to about 0.003 inch thickness. The discs were subsequently jet polished to perforation at room temperature using a solution of 400 ml CH_3COOH + 75 g Cr_2O_3 + 21 ml H_2O and polishing conditions of 30V and 20mA.

3.2.2 TEM Conditions

Substructure characteristics were observed in a Philips EM 301 Transmission Electron Microscope. The accelerating voltage was 100kV. All photos were taken under bright field conditions.

4. Results and Discussion

4.1 TEM Observations: Substructure Development at Room Temperature and -100°C

Substructure development during deformation was characterized using transmission electron microscopy. Representative bright field images of substructures formed after 5% and 10% strain at -100°C are shown in Figures 2a and 2b, respectively. The substructure appearance after deformation to failure at -100°C is shown in Figure 2c. After 5% strain at -100°C (Figure 2a), dislocations are randomly distributed. Many of the dislocations are long and straight, and they are often aligned parallel to one another. After 10% strain at the same temperature (Figure 2b), dislocation segments appear to be shorter, and the dislocation density is higher but still fairly evenly distributed. In specimens deformed to failure at -100°C (Figure 2c), dislocations are gathered into a roughly cellular structure; however, the cell walls are diffuse and many dislocations can be seen in the interior of the cells. This sequence is similar to that observed in iron (Keh and Weissmann, 1963) as discussed in earlier sections.

Bright field images of typical substructures seen in specimens deformed to RTFS-5% and RTFS-10% at room temperature are shown in Figures 3a and 3b, respectively. Representative images of substructures found after deformation to failure at room temperature are shown in Figure 3c. At RTFS-5%, or approximately 4% strain (Figure 3a), the beginnings of cell formation are already visible. The dislocations are not randomly distributed, but are gathered in certain areas, leaving other areas fairly clear. At RTFS-10%, or approximately 7.5% strain (Figure 3b), the dislocation density is higher, and in some areas cell walls are becoming quite pronounced; however, the cell structure is not yet fully developed in all areas. At failure (Figure 3c) the substructure consists of very

well-developed cell walls. The interiors of the cells are nearly clear of dislocations. This behavior is also similar to that observed in iron (Keh and Weissmann, 1963).

In summary, although the dislocation substructures are not fully developed by RTFS-5% or RTFS-10%, there are distinct differences in the dislocation arrangements between specimens deformed to these levels at -100°C and room temperature. Despite difficulties in imaging and photographing the substructure, in general the TEM characterization indicated that the substructure developed during deformation at -100°C was on the whole much more uniformly distributed than that formed at room temperature. The cells that eventually formed at -100°C were more diffuse than those that formed at room temperature. Based on TEM observations, the assumption that the substructures formed at these two temperatures are different seems to be valid.

Additional TEM characterization was performed on two specimens from the interrupted temperature tests. Figure 4a shows the substructure developed after 10% strain at -100°C, followed by deformation to failure at room temperature. The dislocations appear to be arranged in well-formed cells with fairly clean cell interiors. This arrangement is similar to that which forms if the entire deformation is performed at room temperature (see Figure 3c). The substructure shown in Figure 4b was developed during deformation to RTFS-10% at room temperature, followed by deformation to failure at -100°C. In this case the cell structure is somewhat "messier," with more dislocations remaining in the cell interiors. Comparison of Figure 4b with Figure 2c, in which all of the deformation was performed at -100°C, shows that when some of the deformation is performed at room temperature, the cell walls seem somewhat more defined. This indicates that the cell structure that was partially formed in the early room temperature deformation of the specimen shown in Figure 4b persisted after the temperature was lowered, and the -100°C structure was superimposed on this. In summary, these observations indicate that when the temperature is sufficiently high to allow easy dislocation movement, the dislocations will arrange into well-developed cells. This cell structure will persist through further

deformation. However, when the temperature is not high enough to allow this, the dislocations will form a more diffuse, randomly-distributed structure. These observations are also in agreement with similar experiments on iron by Keh and Weissmann (1963).

4.2 Mechanical Behavior

The results of tensile tests done at both constant temperature (room temperature and -100°C) and interrupted temperature (-100°C / R.T. and R.T. / -100°C) are given in Figures 5 - 10. Note that these plots are engineering stress / strain plots. Engineering stress and strain were used in this study rather than true stress and strain because the considerable amount of post-necking elongation that occurs in these specimens limits the validity of the true stress and strain data to the early portion of the tests. Also the use of engineering stress and strain enable straightforward determination of the onset of necking.

Some mention of the processing of this data is in order. The plots pictured in Figures 5 - 10 were calculated using the programs in Appendix 1. These plots were not smoothed. It was found that, because of the relatively small number of data points, smoothing operations tended to obscure the features of the curves. Since considerable smoothing is necessary before accurate slopes can be calculated, the slopes calculated from these plots were very irregular and not appropriate for analysis.

Since the sheet material used in this study exhibits a large amount of elongation after the onset of diffuse necking (i.e. beyond the point of maximum load), it was found that even the use of engineering stress-strain plots above the point of maximum load was somewhat confusing. The stress-strain curve itself is a macroscopic measurement of specimen behavior. Before the point of maximum load the specimen can be assumed to deform uniformly, and the stress-strain curve can be used as an indicator of local behavior. However, beyond maximum load the deformation is no longer uniformly distributed through the gage section, but is concentrated in the neck region; in this case the stress-

strain curve does not necessarily describe local behavior, but is indicative of the behavior in the neck region only. Therefore since the purpose of this study was to investigate the relationship between the microscopic and macroscopic behavior, the stress-strain plots were truncated to the region below maximum load where such a comparison is valid. The determination of the point of maximum load, or similarly the uniform elongation, was done using the method of Considère (1885), as described by Dieter (1976). The analysis of the effect of dislocation substructure on deformation behavior was based only on engineering stress and strain data up to maximum stress. Although they are not strictly relevant to this study, total elongations for the six specimens are listed in Table 3 and discussed in Section 4.32.

4.21 Comparison of Mechanical Behavior at Constant Temperature

Engineering stress-strain plots for room temperature and -100°C are shown in Figures 5 and 6, respectively. A composite of these plots is shown in Figure 11. Figure 5 shows that at room temperature yielding occurs at approximately 25 ksi and is followed by strong work hardening up to the ultimate tensile strength (UTS), approximately 45 ksi. The UTS, signifying the onset of diffuse necking, occurs at approximately 25% strain. Considerable post-uniform elongation, approximately 15%, occurs after necking begins. Figure 6 shows that at -100°C the yield stress is much higher, approximately 55 ksi. The specimen then work hardened weakly up to the UTS at approximately 64 ksi and 15% strain. In this specimen a large amount of post-uniform elongation was also observed.

As can be seen from Figure 11, the deformation behavior differs greatly between the two testing temperatures. However, this difference cannot be directly attributed to differences in dislocation substructure because of the variation in deformation mode between the two temperatures. As previously mentioned, cross-slip is fairly easy at room temperature but severely limited at -100°C. Differences in elastic modulus and friction

stress at the two temperatures may also contribute to the variation in mechanical behavior, as well as to the substructure formation.

4.22 Mechanical Behavior of Specimens Deformed First at -100°C, then at Room Temperature

Figures 7 and 8 show the tensile behavior of specimens deformed first at low temperature, then at room temperature. The specimens of Figures 7 and 8 were deformed to 5% and 10% strain, respectively, at -100°C, warmed to room temperature, then deformed to failure. As is described in Section 4.1, the substructure that evolves during these sequences is characterized by no cell formation during the -100°C straining, followed by cell formation during room temperature straining.

To compare the behavior of specimens with and without cell structure at room temperature, Figures 7 and 8 (tests begun at -100°C and completed at room temperature) can be compared to Figure 5 (test done entirely at room temperature). These plots should not be compared at equivalent strain, but at equivalent flow stress since the RTFS (room temperature flow stress) is assumed to be the state parameter. Since less strain is required at room temperature than at -100°C to attain a given RTFS level, Figure 5 can be shifted along the strain axis so that the beginning of the room temperature behavior in Figures 7 and 8 corresponds with the point of equivalent flow stress on Figure 5. This operation has been performed to obtain the composite curves shown in Figures 12 and 13.

Figures 12 and 13 show that the prestrains of 5% and 10% at -100°C had little effect on the subsequent room temperature behavior of the specimens. Variations in the UTS and necking strain were minimal and within the accuracy of the plots. This behavior will be discussed in Section 4.31. As shown in Table 3, a small decrease in the post-uniform elongation was evident and will be discussed in Section 4.32.

The plots shown in Figures 7 and 8 were used to determine the RTFS values associated with 5% and 10% strain at -100°C. Using the plot in Figure 7, RTFS-5% was determined as the measured flow stress immediately after yielding occurred when the test was continued at room temperature. RTFS-10% was determined similarly from Figure 8. These RTFS values were used as the temperature change points for the tests involving initial deformation at room temperature, followed by continued deformation at -100°C (described in Section 4.23).

4.23 Mechanical Behavior of Specimens Deformed First at Room Temperature, then at -100°C

Figures 9 and 10 show the tensile behavior of specimens deformed first at room temperature, then at -100°C. The specimens of Figures 9 and 10 were deformed to RTFS-5% and RTFS-10%, respectively, at room temperature, cooled to -100°C, then deformed to failure. As is described in Section 4.1, the substructure that evolves during these sequences is characterized by cell formation during the room temperature straining, followed by a small amount of dislocation agglomeration in the cell interiors during -100°C straining.

To compare the behavior of specimens with and without cell structure at -100°C, Figures 9 and 10 can be compared to Figure 6 (the -100°C tensile test). Again the RTFS should be used as the state parameter. Since the temperature changes in the tests were performed at the RTFS corresponding to 5% and 10% strains at -100°C, the plot in Figure 6 can be shifted along the strain axis so that the 5% and 10% strain points line up with the temperature changes in Figures 9 and 10, respectively. This operation has been performed to obtain the composite curves shown in Figures 14 and 15.

Figures 14 and 15 show that the room temperature prestrains had little effect on the subsequent -100°C mechanical behavior. UTS and uniform elongation values varied only

minimally. This behavior will be discussed in Section 4.31. Table 3 shows that the prestrained samples exhibited significantly less total elongation; this behavior will be discussed briefly in Section 4.32.

4.3 Effect of Substructure on Mechanical Behavior

In this section the results reported in the previous section will be discussed. The uniform, or pre-necking, deformation behavior, the primary topic of this study, will be discussed in Section 4.31. The behavior beyond maximum load will be briefly discussed in Section 4.32.

4.31 Pre-Necking Behavior and Implications for Work Hardening Theory

As reported in Sections 4.22 and 4.23, specimens that have been prestrained at different temperatures to induce different dislocation substructures performed similarly under subsequent deformation conditions. This suggests that the dislocation arrangement in this material may have little effect on its deformation behavior, at least in the range of substructures up to well-developed cells. This result agrees with the conclusions of Biswas et. al. (Biswas, Cohen, and Breedis, 1973) from their comparison of the behavior of titanium alloys of different substructure. This result is also in accord with the inability of past investigators to relate the onset of certain types of substructure formation with the various "stages" of work hardening.

The apparent irrelevance of substructure has interesting implications for the theory of work hardening. First of all, if the dislocation substructure has no effect on deformation, then it should be possible to formulate a work hardening theory that encompasses the entire range of substructure development through cell formation. In this

case existing theories that apply to only one phase of substructure evolution (for example, to cellular structures only) should be extended to non-cellular structures.

However, before any influence of substructure is ruled out completely, some caution is necessary. The effect of grain boundaries on material strength is well known. In a microscopic sense, grain boundaries can be viewed as well-developed cell walls of high dislocation density and misorientation. Since grain boundaries have a significant effect on mechanical behavior, it seems reasonable to expect that a well-developed cell structure could have some bearing on deformation behavior. Work by Langford and Cohen (1975) suggests that in the latter stages of cell development, when large misorientations between cells are observed, the cell walls may begin to take a more active role. They postulated the existence of a "critical misorientation between adjacent cells" above which dislocations can no longer pass through the cell walls. In this case the substructure would have some effect on work hardening behavior if the flow stress is propagation-controlled. Unfortunately the effect of this type of substructural development on mechanical behavior cannot be observed by the methods used in this study because the onset of necking would preempt the formation of the substructures of interest. Perhaps alternate deformation conditions, such as torsion or wire drawing, which allow large strains before necking, could be used.

The results of this study also cast some doubt on the validity of "propagation-controlled flow stress" models of work hardening for the range of substructures studied. It seems that dislocation cell walls, regardless of how small their misorientation, would act as much different barriers to dislocation motion than the same density of dislocations randomly assembled. Since no particular change in stress-strain behavior can be traced to a change in substructure, mechanisms that assume that the flow stress is controlled entirely by dislocation propagation seem somewhat questionable.

In contrast, the "multiplication-controlled flow stress" models are based on the stress needed to activate the weakest dislocation source, be it a dislocation link or tangle, a cell wall, or elsewhere. It seems conceivable that the differences in the strengths of these

types of sources could be rather small, and that the sources in one type of substructure could be just as effective as those in another type. For this reason the "multiplication-controlled flow stress" type models are given more credibility by the results presented here.

4.32 Post-Uniform Deformation Behavior

As shown in Table 3, the -100°C prestrains seem to have little effect on room temperature mechanical behavior after necking, while the room temperature prestrains seem to have a significant effect on subsequent -100°C post-necking behavior. This effect is very interesting, especially from the viewpoint of formability. If the total elongation can somehow be altered by controlling the dislocation substructure, improvements in formability could be significant.

Interpretation of this result is made difficult by two factors. One problem stems from the fact that post-uniform deformation behavior does not depend only on the "microscopic" (i.e. dislocation scale) behavior, but also on the "macroscopic" behavior of large defects. Ghosh (1977) has shown that factors such as strain rate sensitivity, anisotropy, and defect size have strong effects on the behavior in this strain regime. The second problem arises because of the test procedure used. The tests described here were designed to allow direct correlation between deformation behavior and substructure. However, after the onset of necking, the measured behavior is no longer an accurate description of local behavior because of the localization of deformation in the neck region. It is thus difficult to draw any conclusions about the effect of substructure on deformation behavior in this region. Since the results reported here are based on a limited test matrix, and emphasis was not placed on the above concerns, conclusions on post-uniform behavior would be very speculative. However, future study in this area, with a sufficiently large test matrix to produce good statistics, could prove very interesting.

4.4 Evaluation of Room Temperature Flow Stress as a State Parameter for Deformation

In this study the Room Temperature Flow Stress (RTFS) was used as a state parameter for deformation, rather than the usual strain. The reasons for this choice are explained in Section 2.22. To review, this parameter was viewed as a measure of the resistance of the material to the forces applied when the amount of thermal activation was held constant. From this point of view, the -100°C Flow Stress or the Mechanical Threshold Stress (flow stress at zero Kelvin) would be equally good choices; RTFS was chosen for experimental convenience. In addition if the RTFS is indeed an appropriate state parameter, then for the same tests the -100°C Flow Stress should also be a state parameter.

Recalling the test procedure, one specimen was first deformed to a given strain (5% or 10%) at -100°C, then deformed at room temperature, as shown in Figures 7 and 8. To define the state of the material at the point of this temperature change, the plots shown in Figures 7 and 8 were used to determine the RTFS associated with the given amount of -100°C deformation; the RTFS was defined as the yield stress at the beginning of the room temperature portion following the given -100°C strain. In the opposite temperature sequence tests, the specimens were deformed first to the appropriate RTFS (as previously determined), then chilled and deformed at -100°C, as shown in Figures 9 and 10. Thus the RTFS values for the two sets of tests were forced to coincide by the test procedure.

Figure 16 shows a composite of the plots from the two tests in which the temperature change occurred at RTFS-5% (from Figures 7 and 9); Figure 17 is a similar composite for RTFS-10% (from Figures 8 and 10). These plots show that indeed the RTFS values match between the two tests, as they are forced to do by the test procedure.

As described in the first paragraph in this section, if the RTFS if an appropriate state parameter, then the -100°C Flow Stress should also be a good state parameter. The

choice of the RTFS as the state parameter can be evaluated by comparing the -100°C Flow Stresses that correspond to the RTFS values that were set to be equivalent. Figures 16 and 17 show that the two corresponding -100°C Flow Stresses are also in good agreement.

At least for this study the RTFS seems to be a good state parameter. To further evaluate this parameter, a series of tests such as these at a variety of strain levels could be compared to give a better statistical basis. Tests at different strain rates, rather than different temperatures, could similarly be used.

4.5 Implications for Formability

Although the appropriate state parameter to describe deformation seems to be the flow stress at a given temperature, the more important parameter from a metal forming standpoint is the strain. In a sheet forming operation the total amount of strain that a material can accommodate before local necking is of vital interest. Although the strain between the onset of diffuse necking and the onset of local necking can be significant in the steel used in this study, the regime up to the point of diffuse necking (maximum stress) is also important. The results of this study have direct implications in this area. (For a discussion of diffuse and local necking in sheets, see Backofen, 1972.)

Figure 16 shows that the room temperature strain required to attain RTFS-5% is approximately 4%, with 7% required to attain RTFS-10%. In other words, because work hardening is stronger at room temperature than at -100°C, less strain is required at room temperature compared to at -100°C to reach an equivalent flow stress. This difference in work hardening rates between the two temperatures is also evident in Figure 11.

The deformation process up to necking can be seen as a competition: as necking approaches, the material's satisfactory performance depends on its ability to work harden to distribute the applied stress and avoid localization. But if the material work hardens very strongly from the beginning, it will rapidly approach the maximum stress and the onset of

necking. This presents a quandary, in that the ideal material for forming would work harden weakly at first (to keep the stress level low), then work harden strongly as necking approaches (to avoid strain localization).

As mentioned above, the work hardening rate at -100°C is much lower than at room temperature. This result suggests that if the material is prestrained at -100°C to some point below the necking strain for that temperature before straining at room temperature, more pre-necking strain can be obtained than if the entire deformation process was performed at room temperature. Comparison of Figure 5 (-100°C) with Figures 7 and 8 (-100°C / RT tests), without adjusting the strain axis to get equivalent flow stresses, indicates that this increase in uniform strain is obtainable.

Although the experimental difficulties preclude the immediate application of this procedure to industrial processes, the result indicates some promise. For instance, since a decrease in deformation temperature is often considered equivalent to an increase in strain rate, the same result might be obtainable by varying the strain rate over the course of a forming operation. This approach might be more workable and should be investigated more fully.

5. Conclusions

A study of the mechanical behavior of sheet tensile specimens of low carbon AK DQ steel with different dislocation substructures has shown that the dislocation configuration apparently has little influence on the mechanical behavior up to the point of necking. Using the Room Temperature Flow Stress (RTFS) as the state parameter for deformation, specimens were prestrained to an equivalent RTFS at room temperature and -100°C, developing cellular and non-cellular substructures, respectively. These specimens were subsequently deformed further at a single temperature, so that their mechanical behavior could be compared. Variations in the ultimate tensile strengths and uniform elongations of the specimens were found to be minimal, despite the difference in dislocation configuration. The implications of the apparent unimportance of substructure to deformation behavior have been discussed, especially with respect to current work hardening theory.

In these experiments the allowable range of strains that could be studied was limited by the early onset of diffuse necking in the uniaxial tensile test. To study the effect of dislocation substructure at large strains, in the regime of subgrain formation, different mechanical test conditions, such as torsion, rolling, or wire drawing, should be employed.

One aspect of this work has interesting application to sheet formability. Because work hardening in this material is much higher at room temperature than at -100°C, more strain is required at the lower temperature to reach the same room temperature flow stress. This effect could be used to increase the total uniform deformation achieved before the onset of necking. If a specimen was prestrained at low temperature to some point below the ultimate tensile stress, then further formed at room temperature, the work hardening rate would be kept low at the beginning of the test, keeping the flow stress low in the initial portion of the forming process; then in the latter part of the process, when the material must work harden strongly to avoid the onset of necking, the room temperature

deformation would provide a high work hardening rate. Although these large temperature variations may not be feasible for commercial forming processes, a similar effect could be obtained by starting with a higher strain rate (analogous to lower temperature), then finishing with a lower strain rate (analogous to higher temperature).

In the post-uniform deformation regime, significant variation in behavior between the different substructure specimens was observed. While the -100°C prestrain (to develop a non-cellular substructure) seemed to have little effect on the total elongation, the room temperature prestrain (to develop a cellular substructure) reduced the total elongation by more than 10% strain. However, it is not clear whether this effect is a result of differences in substructure, or merely a result of some macroscopic variation in the specimens. Further study in the regime of necking is highly recommended.

The experimental procedure used in this study utilized the Room Temperature Flow Stress (RTFS) as the state parameter for deformation, rather than the conventional parameter, strain. Evaluation of this parameter was done based on the principle that if the RTFS is a good state parameter, then specimens of equivalent RTFS should also have equivalent flow stress at other temperatures. It was found that specimens of equal RTFS also had the same -100°C Flow Stress, indicating that the RTFS is an appropriate state parameter for deformation. As most past and current experiments assume that strain is the appropriate state parameter, this successful use of the flow stress at a given temperature as a measure of equivalently deformed states is an important result.

References

Ashby, M. F. (1966), *Acta Metall.*, vol. 14, pg. 679.

Backofen, W. A. (1972), *Deformation Processing*, Addison-Wesley, Reading, MA, pg. 204.

Biswas, C., Cohen, M. and Breedis, J. F. (1973), "Strain Hardening of Titanium by Severe Plastic Deformation," *The Microstructure and Design of Alloys*, vol. I, Proc. 3rd Int. Conf. on the Strength of Metals and Alloys (ICSMA3), Cambridge, pp. 16-20.

Brown, L. M. and Ham, R. K. (1971), *Strengthening Methods in Crystals*, A. Kelly and R. B. Nicholson, eds., Applied Science, London, pg. 12.

Considère, A. (1885), *Ann ponts et chaussées*, vol. 9, ser. 6, pp. 574-775.

Dieter, G. E. (1976), *Mechanical Metallurgy*, McGraw-Hill, New York, pp. 342-344.

Follansbee, P. S. (1986), "High-Strain-Rate Deformation of FCC Metals and Alloys," *Metallurgical Applications of Shock-Wave and High-Strain-Rate Phenomena*, L. E. Murr, K. P. Staudhammer and M. A. Meyers, eds., Marcel Dekker, Inc., New York, pp. 451-479.

Follansbee, P. S. and Kocks, U. F. (1986), "A Constitutive Description of the Deformation of Copper Based on the Use of Mechanical Threshold Stress as an Internal State Variable," submitted to *Acta Metallurgica*..

Ghosh, A. K. (1977), "A Numerical Analysis of the Tensile Test for Sheet Metals," *Met Trans*, vol. 8A (August 1977), pp. 1221-1232.

Gil Sevillano, J., van Houtte, P., and Aernoudt, E. (1980), "Large Strain Work Hardening and Textures," *Prog Mat Sci*, v. 25, no. 2-4, J. W. Christian, P. Haasen and T. B. Massalski, eds., pp. 239-266.

Hirsch, P. B. and Mitchell, T. E. (1968), *Work Hardening*, J. P. Hirth and J. Weertman, eds., Gordon and Breach, New York, pg. 65.

Keh, A. S. and Weissmann, S. (1963), "Deformation Substructure in Body-Centered Cubic Metals," *Electron Microscopy and Strength of Crystals* , G. Thomas and J. Washburn, eds., Interscience, New York, pp. 243-249.

Kocks, U. F., Argon, A. S., and Ashby, M. F. (1975), "Thermodynamics and Kinetics of Slip," *Prog Mat Sci*, vol. 19, B. Chalmers, J. W. Christian and T. B. Massalski, eds.

Kuhlmann-Wilsdorf, D. (1962), *Trans AIME*, vol. 224, pg. 1047.

Kuhlmann-Wilsdorf, D. (1968), *Work Hardening*, J. P. Hirth and J. Weertman, eds., Gordon and Breach, New York, pg. 97.

Kuhlmann-Wilsdorf, D. (1970), *Met Trans*, vol. 1, pg. 3173.

Kuhlmann-Wilsdorf, D. (1977), *Work Hardening in Tension and Fatigue*, A. W. Thompson, ed., AIME, New York, pg. 1.

Kuhlmann-Wilsdorf, D. (1985), "Theory of Workhardening 1934-1984," *Met Trans*, vol. 16A (December 1985), pp. 2091-2108.

Langford, G. and Cohen, M. (1969), *Trans ASM*, vol. 62, pg. 623.

Langford, G. and Cohen, M. (1970), *Met Trans*, vol. 1, pg. 901.

Langford, G. and Cohen, M. (1975), "Microstructural Analysis by High-Voltage Electron Diffraction of Severely Drawn Iron Wires," *Met Trans*, vol. 6A (April 1975), pp. 901-910.

Ledezma, M. (1986), *Three-Dimensional Study of Dislocation Substructures in Punch-Stretched, AK, DQ, Low-Carbon Steel Sheets*, M. S. Thesis, University of California, Berkeley, California.

Li, J. C. M. (1963a), *Trans AIME*, vol. 227, pg. 239.

Li, J. C. M. (1963b), *Electron Microscopy and Strength of Crystals*, G. Thomas and J. Washburn, eds., Interscience, New York, pg. 713.

Li, J. C. M. and Chou, Y. T. (1970), *Met Trans*, vol. 1, pg. 1145.

Morris, J. W., Jr. (1987), course notes: Thermodynamics and Phase Transformations (MSE 201B), Dept. of Mat. Sci. and Eng., University of California, Berkeley, California, pg. 202-203.

Seeger, A. (1957), *Dislocations and Mechanical Properties of Crystals*, J. C. Fisher, W. G. Johnston, R. Thomson and T. Vreeland, Jr., eds., John Wiley and Sons, New York, pg. 243.

Shaffer, S. J. (1986), *The Relevance of Inclusions on Formability in Punch-Stretching of Low-Carbon, AK, DQ Steel*, M. S. Thesis, University of California, Berkeley, California.

Taylor, G. I. (1934), *Proc Roy Soc A*, vol. 145, pg. 362.

Table 1: Mechanical properties of AK DQ steel as supplied by General Motors Corporation

Property	Edge X	Center		Edge Y
	L	L	T	L
Yield Strength (ksi)	24.2	24.3	25.4	22.6
Tensile Strength (ksi)	45.9	46.4	46.6	44.7
Total Elongation (% in 2")	44.0	42.8	37.7	44.1
n Value	.23	.22	.21	.23
Hardness (Rockwell B)	44	43	45	41
r_m	1.55			
Δr	0.48			

Table 2: Chemical composition of AK DQ steel as supplied by General Motors Corporation

Element	C	Mn	P	S	Si	Cu	Ni	Cr	Mo	Sn	Al	N
%	.05	.22	.012	.013	.02	.04	.02	.033	.014	.007	.052	.0091

Table 3: Total Elongation Data

Test	Total Elongation (%)
1	40
2	39
3	41
4	40
5	26
6	28

Key to Test Numbers:

1. Room Temperature Tensile Test
2. -100°C Tensile Test
3. 5% strain at -100°C, continued at room temperature
4. 10% strain at -100°C, continued at room temperature
5. to RTFS-5% at room temperature, continued at -100°C
6. to RTFS-10% at room temperature, continued at -100°C

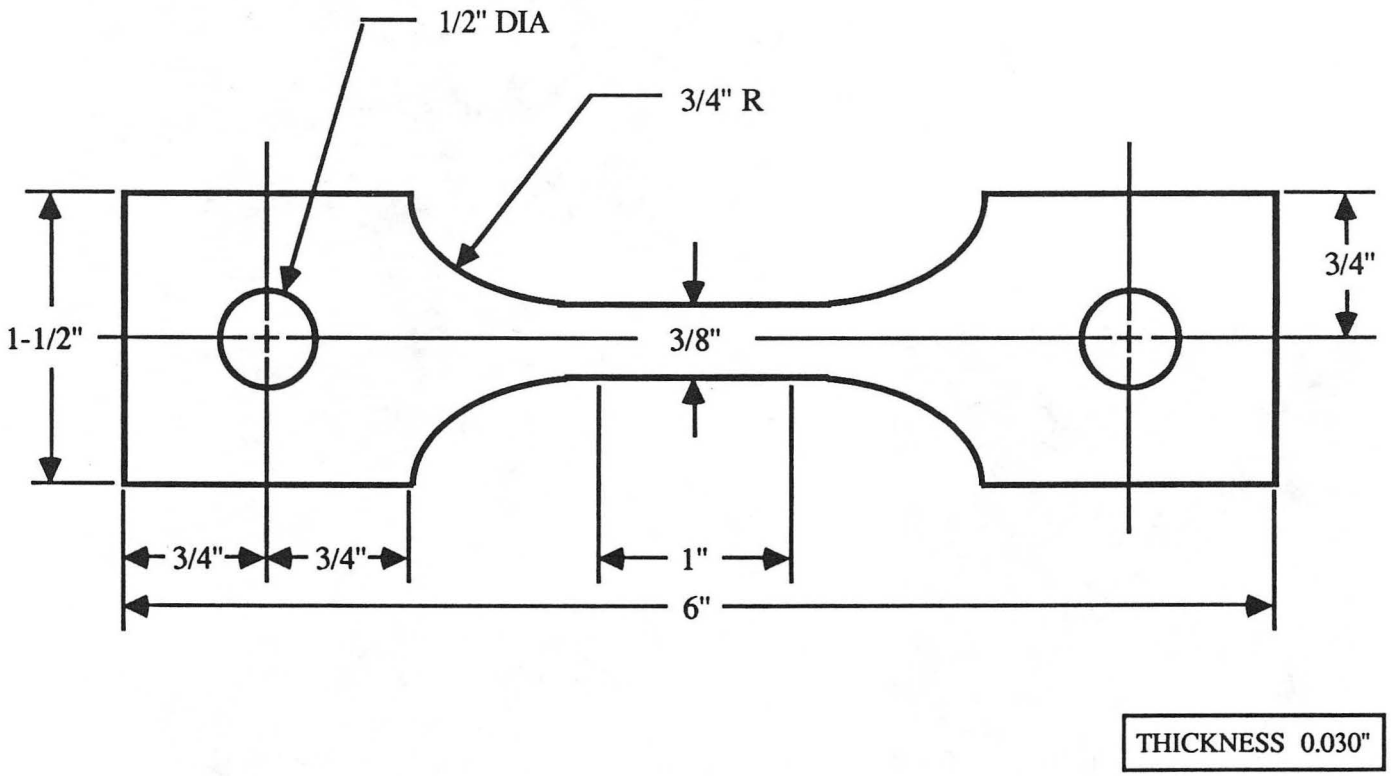

Figure 1. Tensile Specimen Configuration.

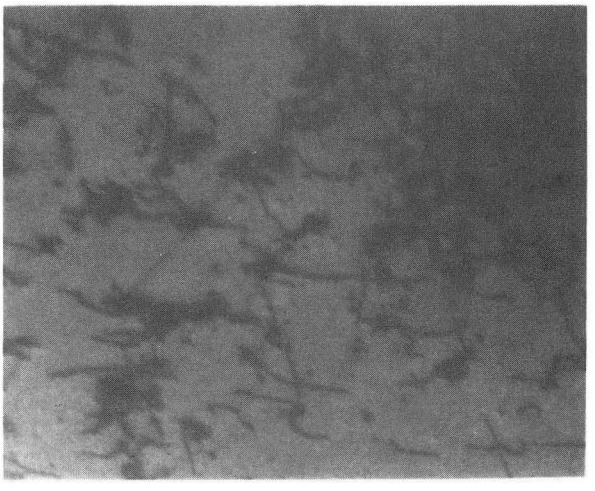

0.5 μm

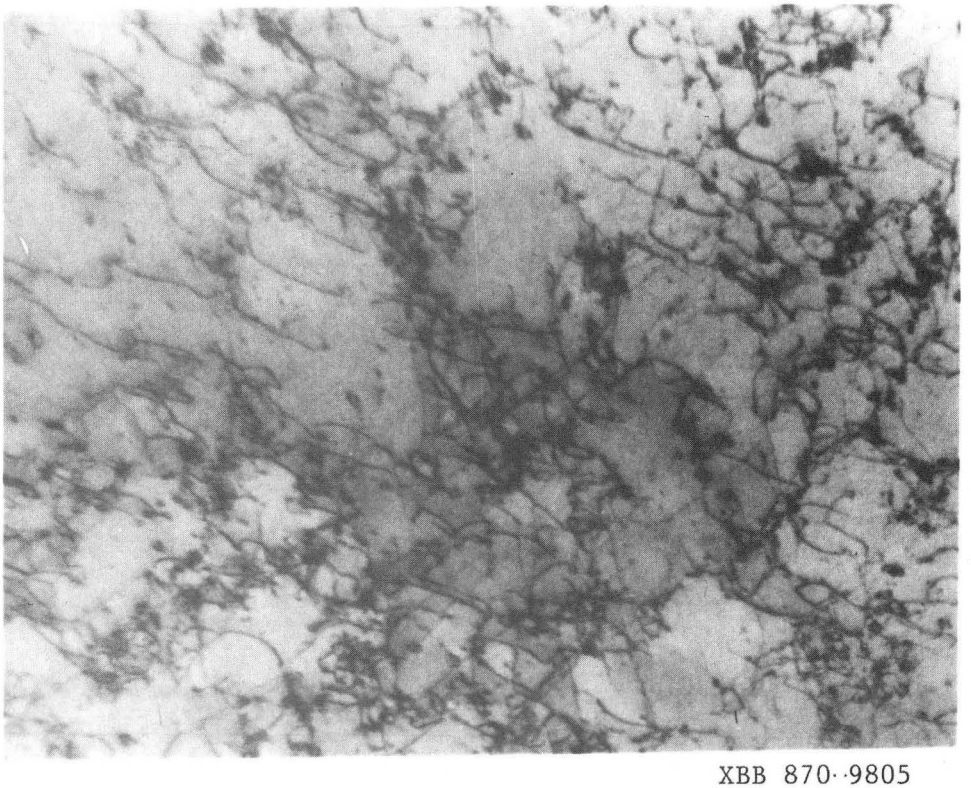

XBB 870··9805

0.5 μm

Figure 2a. TEM bright field images of typical dislocation substructure in specimen deformed to 5% strain at -100°C.

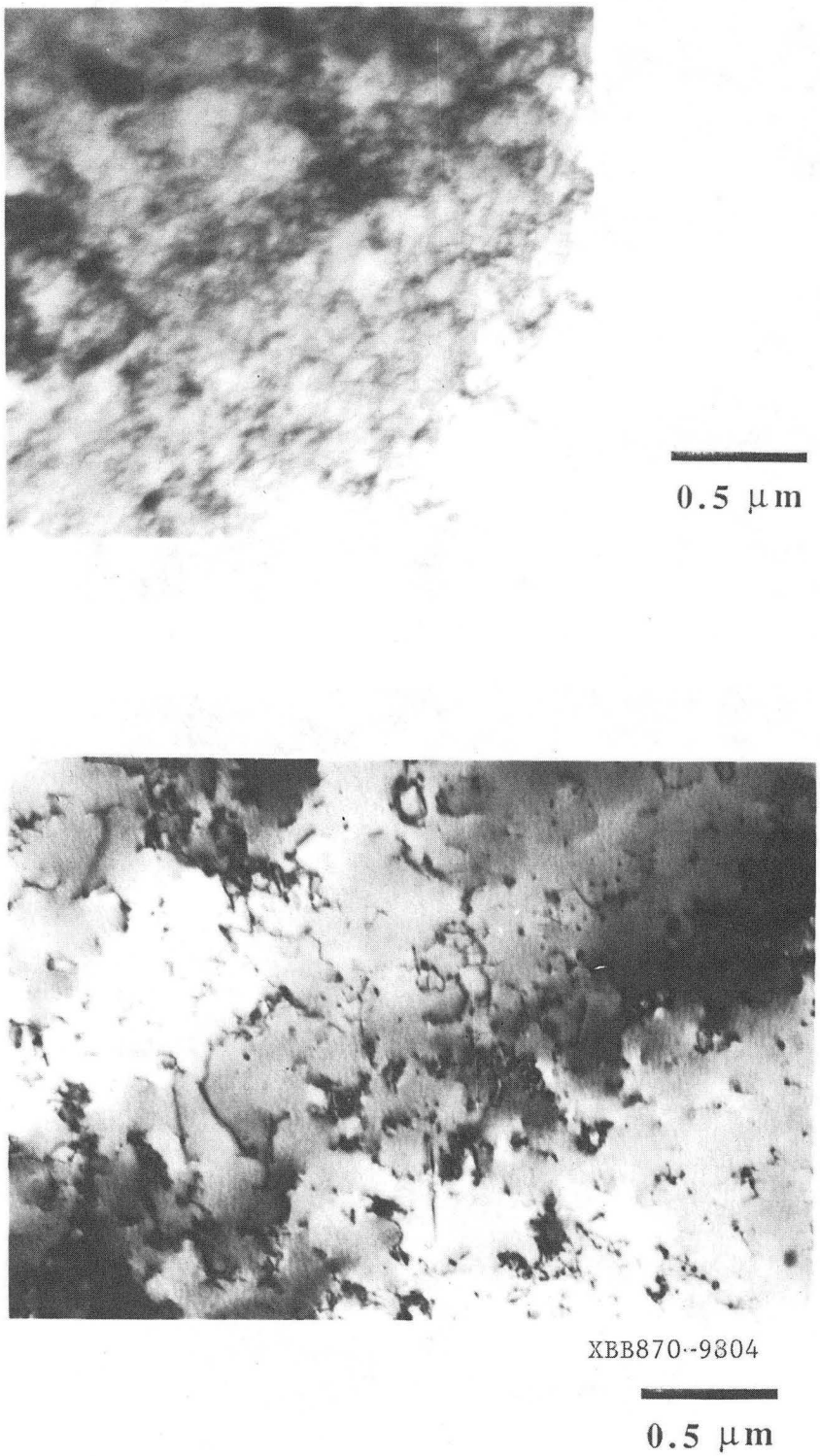

Figure 2b. TEM bright field images of typical dislocation substructure in specimen deformed to 10% strain at -100°C.

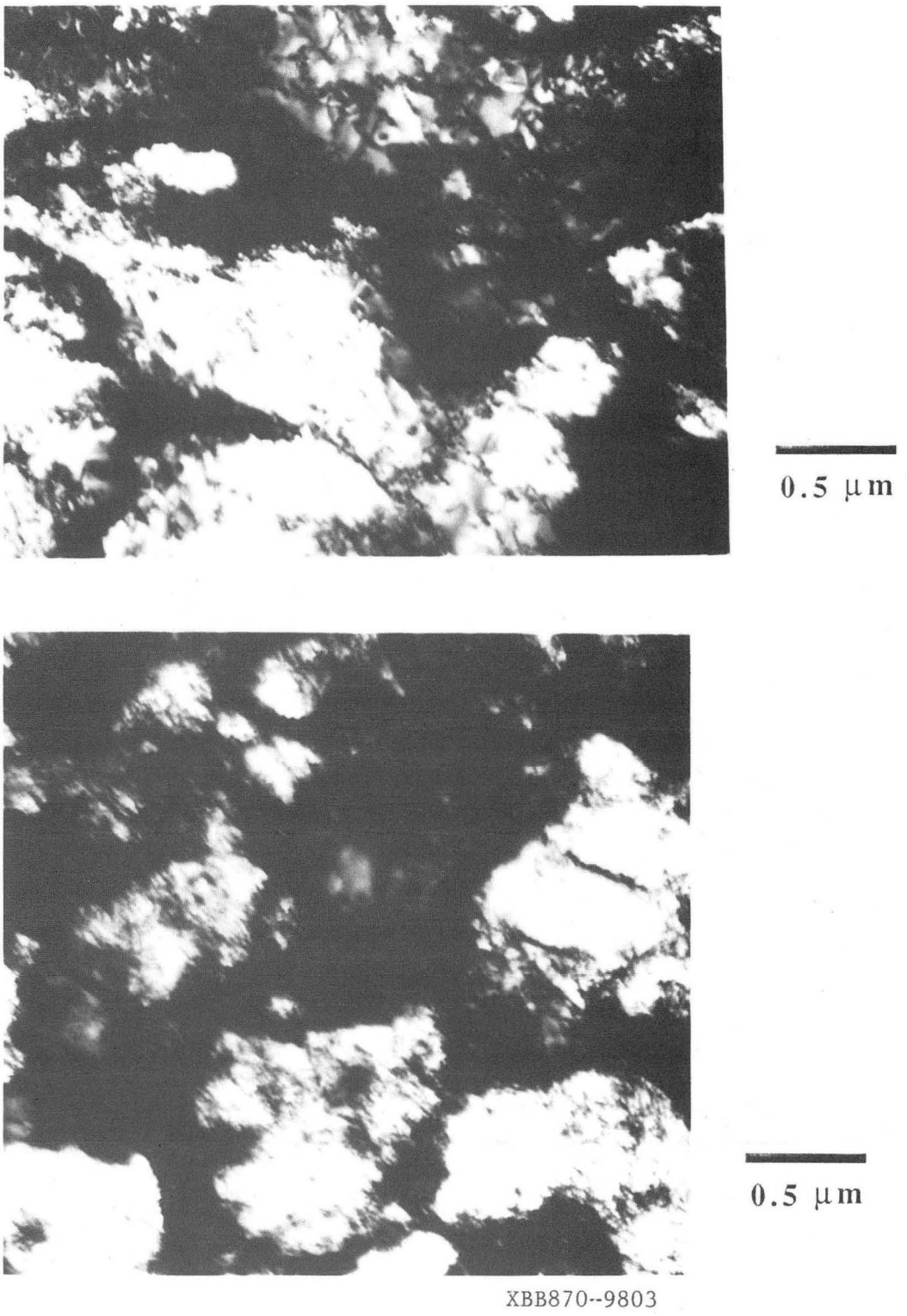

Figure 2c. TEM bright field images of typical dislocation substructure in specimen deformed to failure at -100°C.

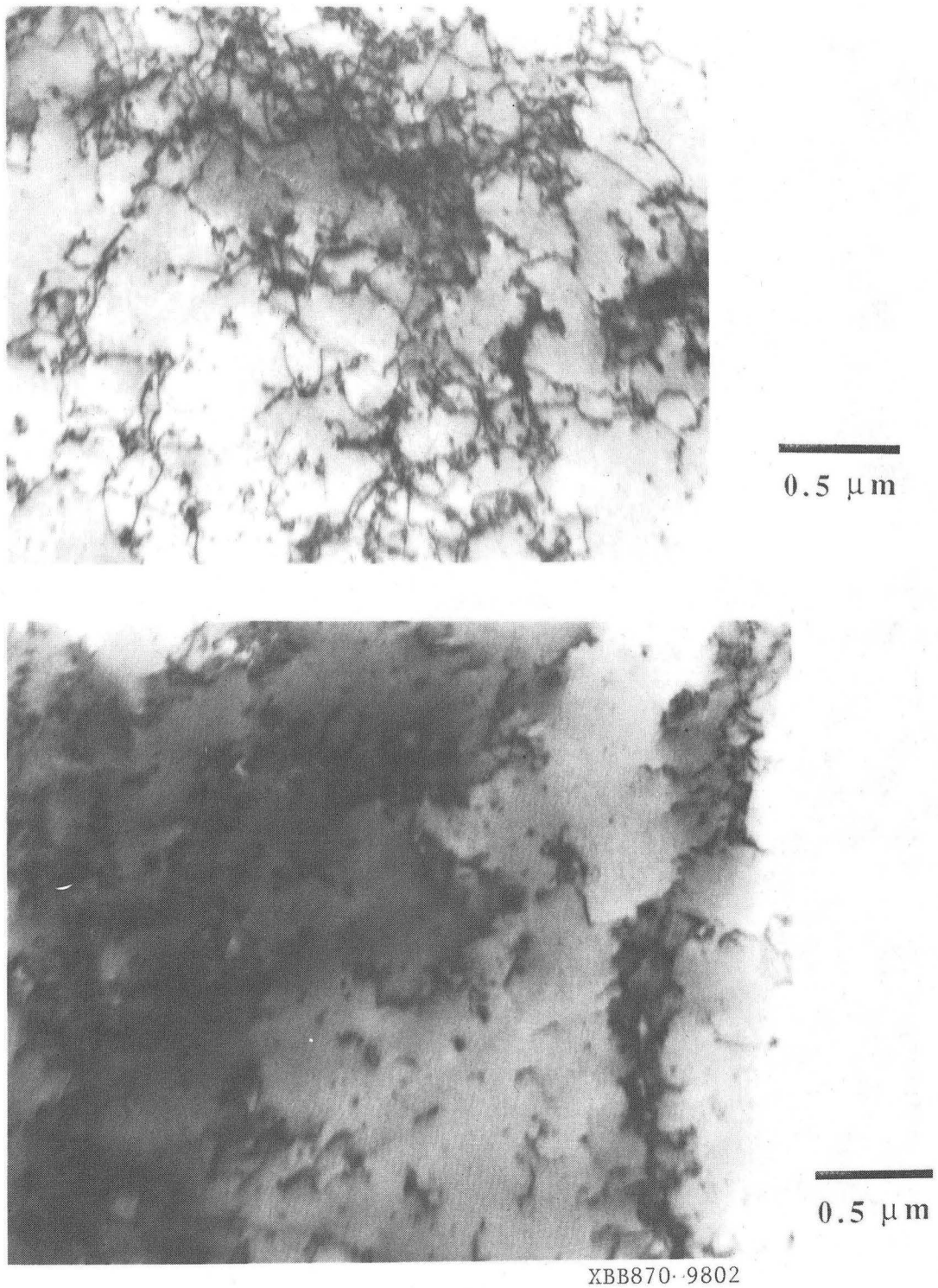

Figure 3a. TEM bright field images of typical dislocation substructure in specimen deformed to RTFS-5% (approximately 4% strain) at room temperature.

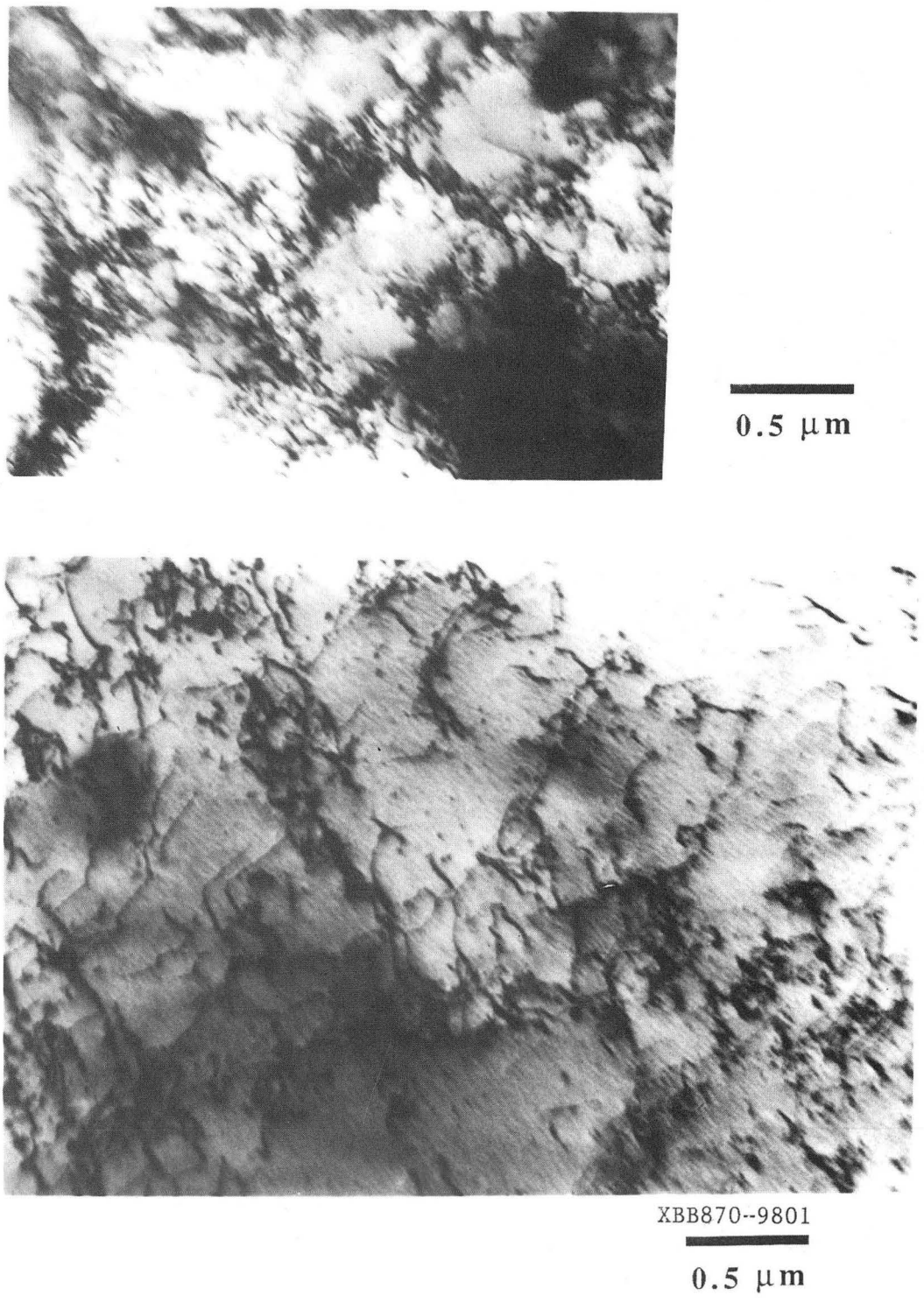

Figure 3b. TEM bright field images of typical dislocation substructure in specimen deformed to RTFS-10% (approximately 7.5% strain) at room temperature.

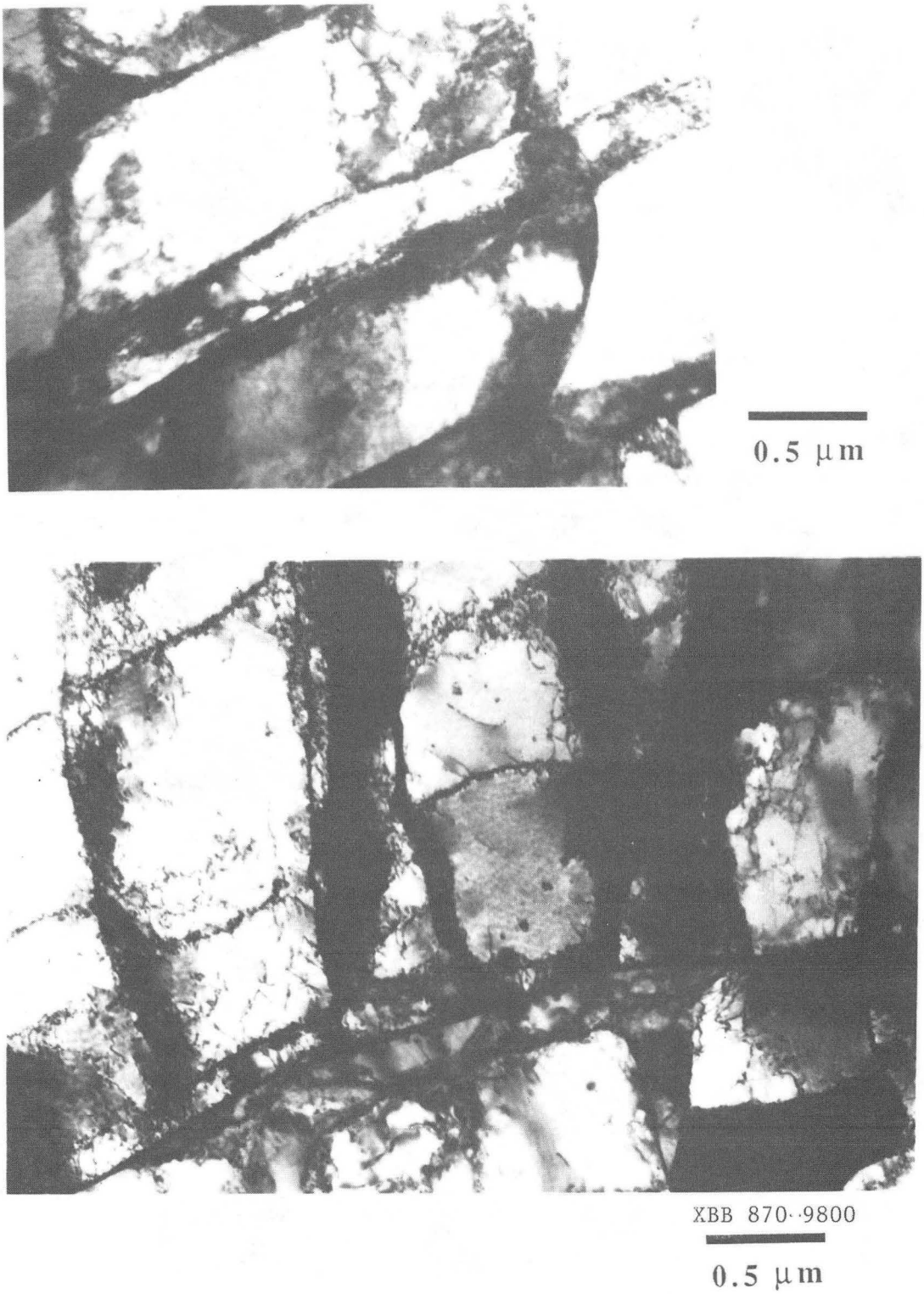

Figure 3c. TEM bright field images of typical dislocation substructure in specimen deformed to failure at room temperature.

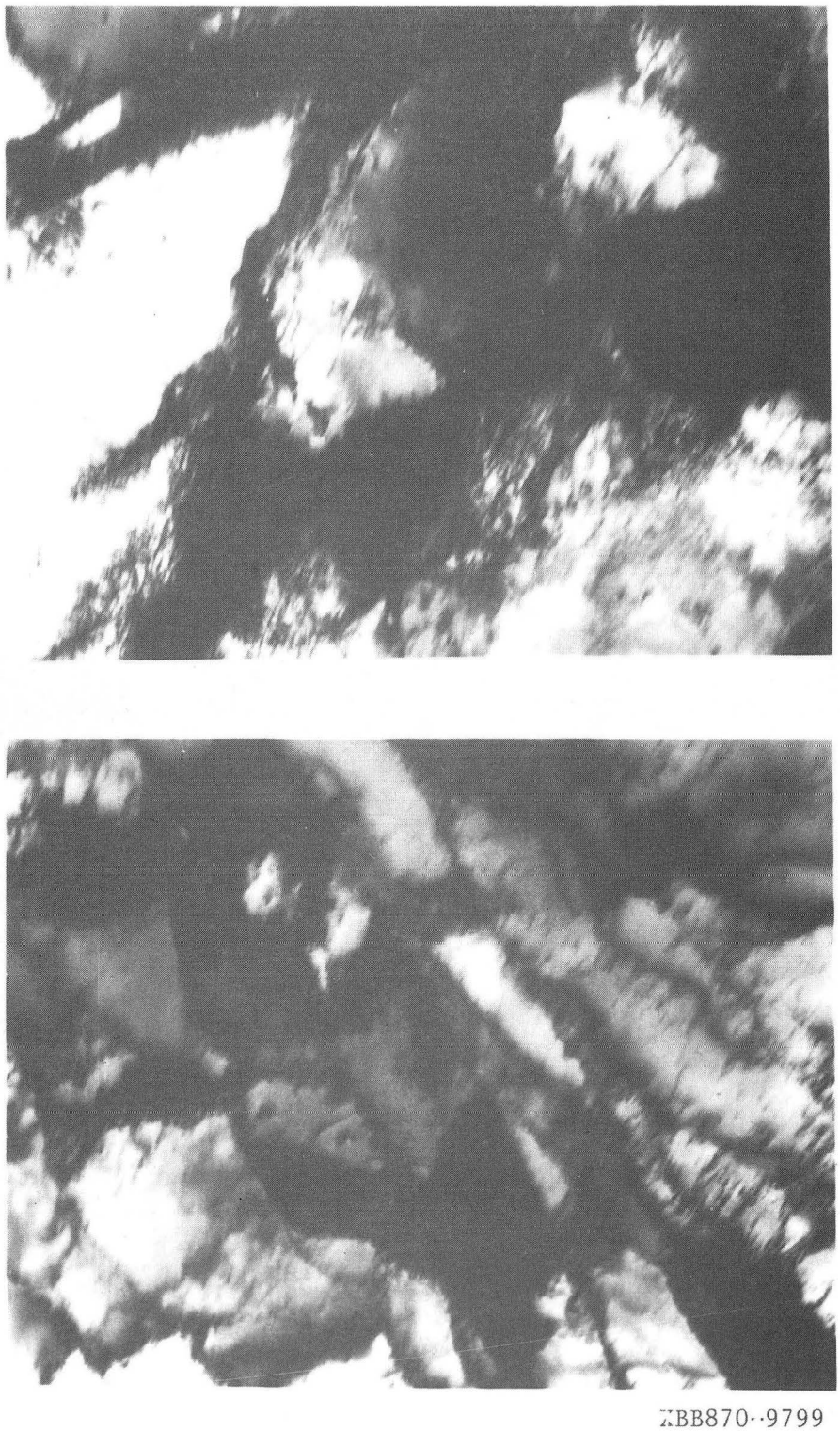

Figure 4a. TEM bright field images of typical dislocation substructure in specimen deformed to 10% strain at -100°C, then deformed to failure at room temperature.

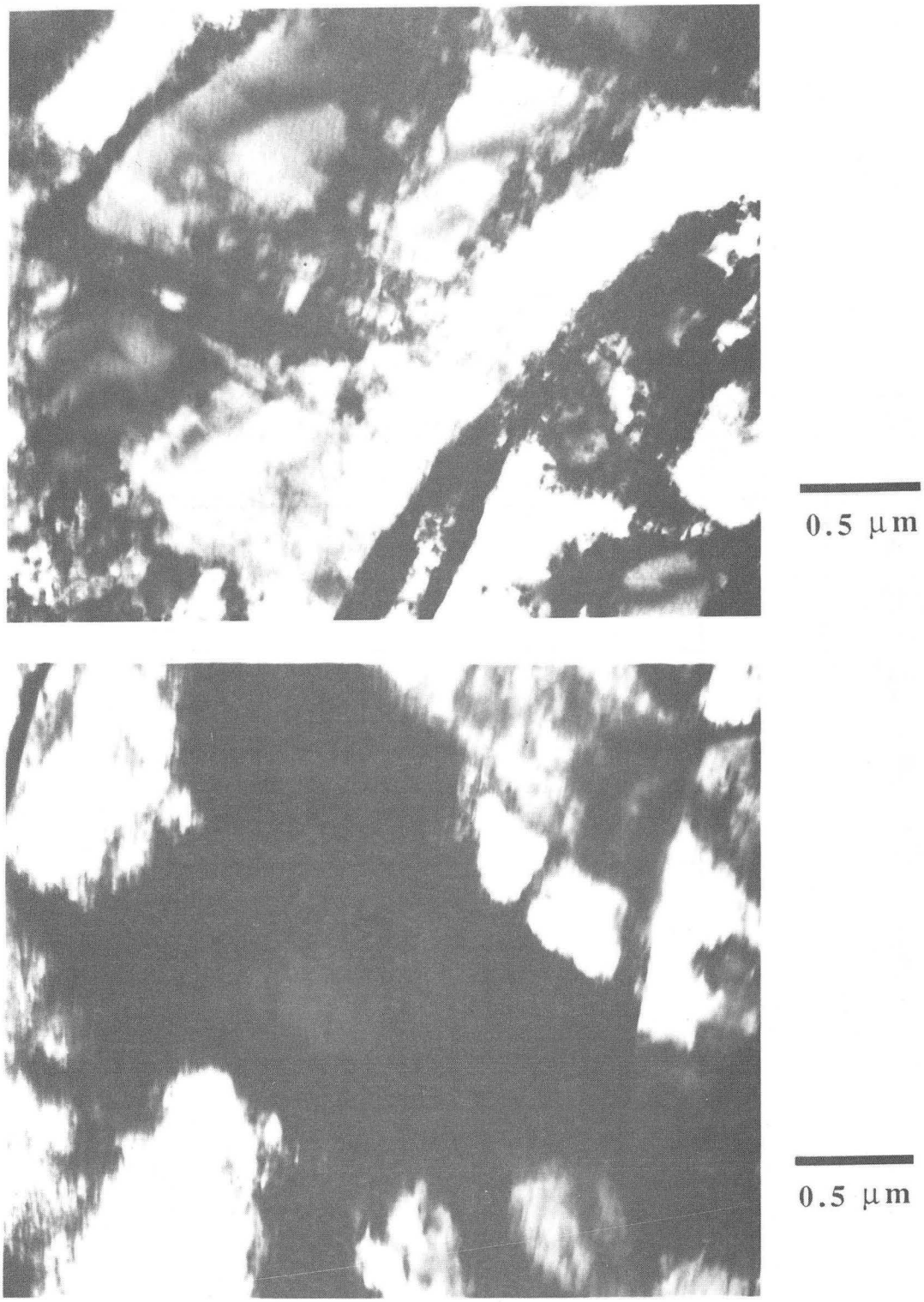

Figure 4b. TEM bright field images of typical dislocation substructure in specimen deformed to RTFS-10% at room temperature, then deformed to failure at -100°C.

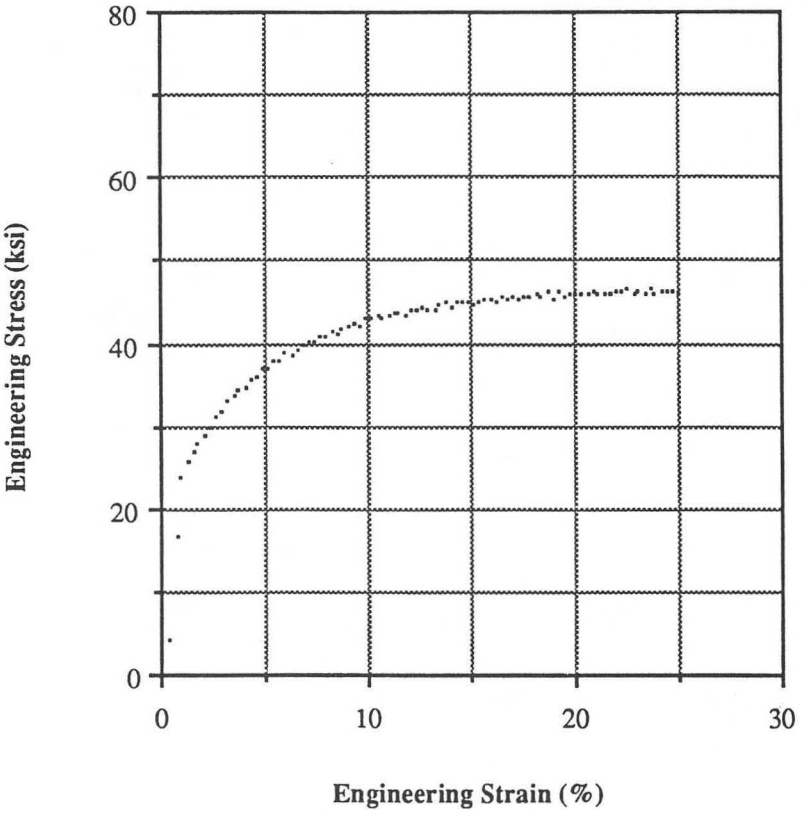

Figure 5. Room temperature tensile behavior.

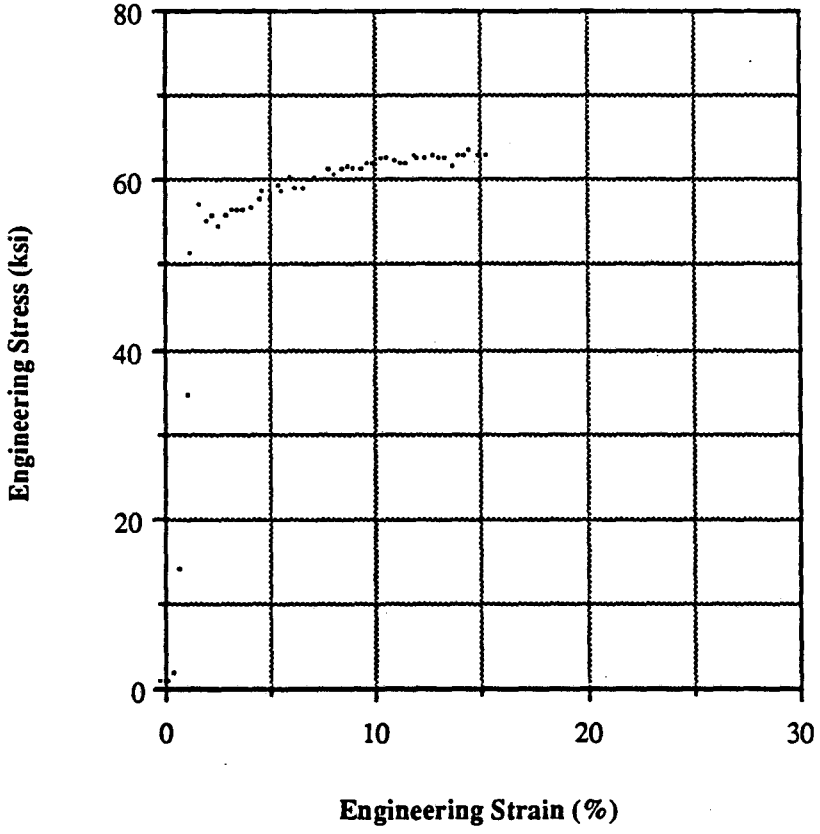

Figure 6. -100°C tensile behavior.

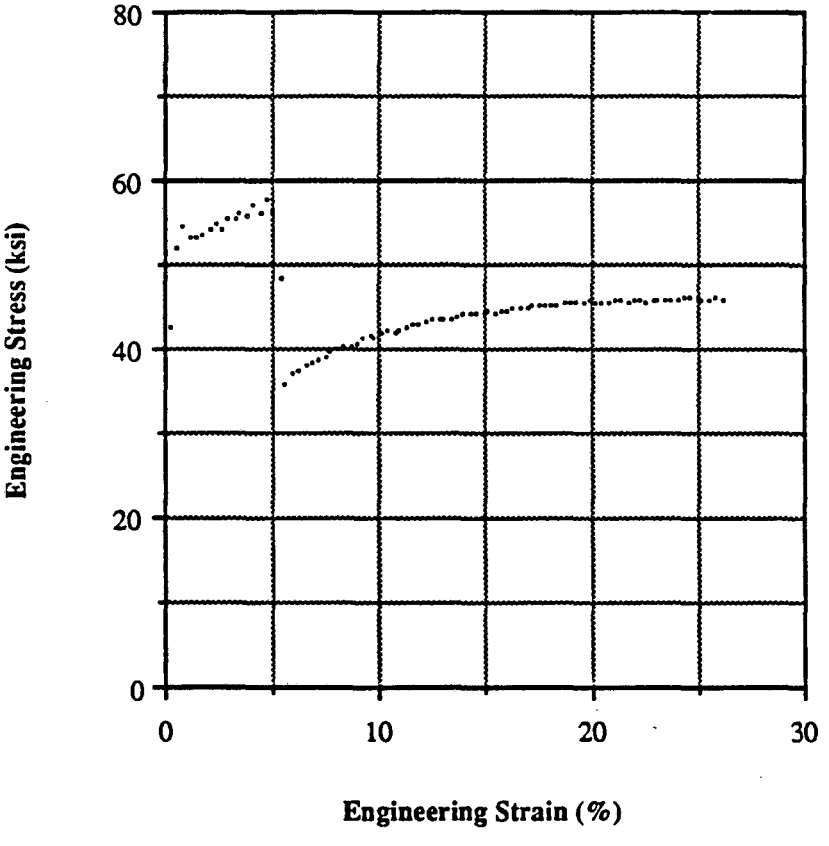

Figure 7. Tensile behavior of specimen deformed to 5% strain at -100°C, then to failure at room temperature.

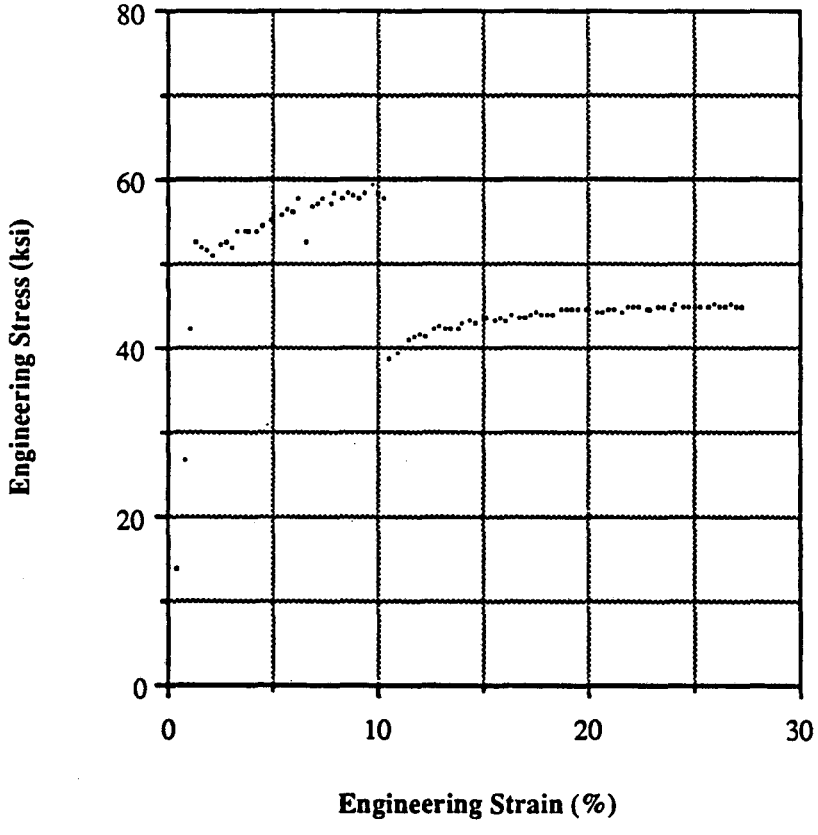

Figure 8. Tensile behavior of specimen deformed to 10% strain at -100°C, then to failure at room temperature.

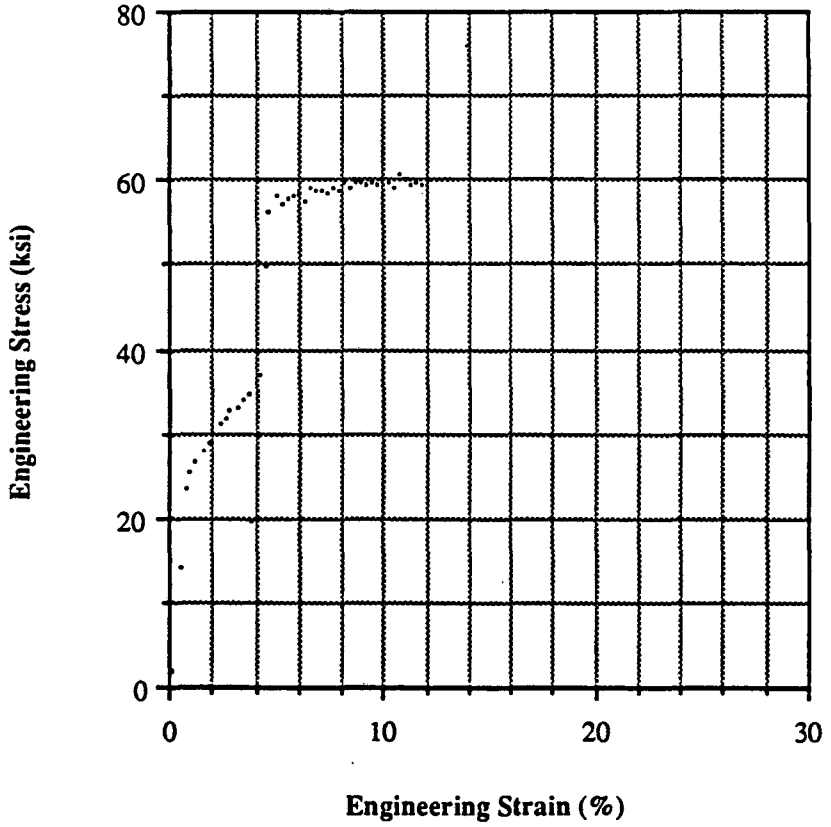

Figure 9. Tensile behavior of specimen deformed to RTFS-5% at room temperature, then to failure at -100°C.

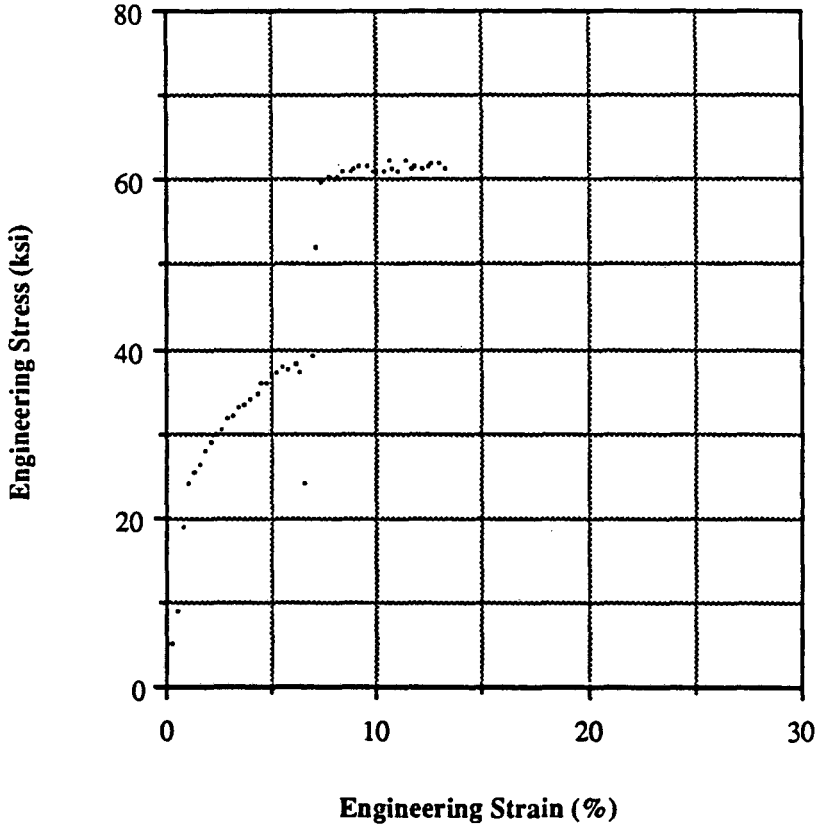

Figure 10. Tensile behavior of specimen deformed to RTFS-10% at room temperature, then to failure at -100°C.

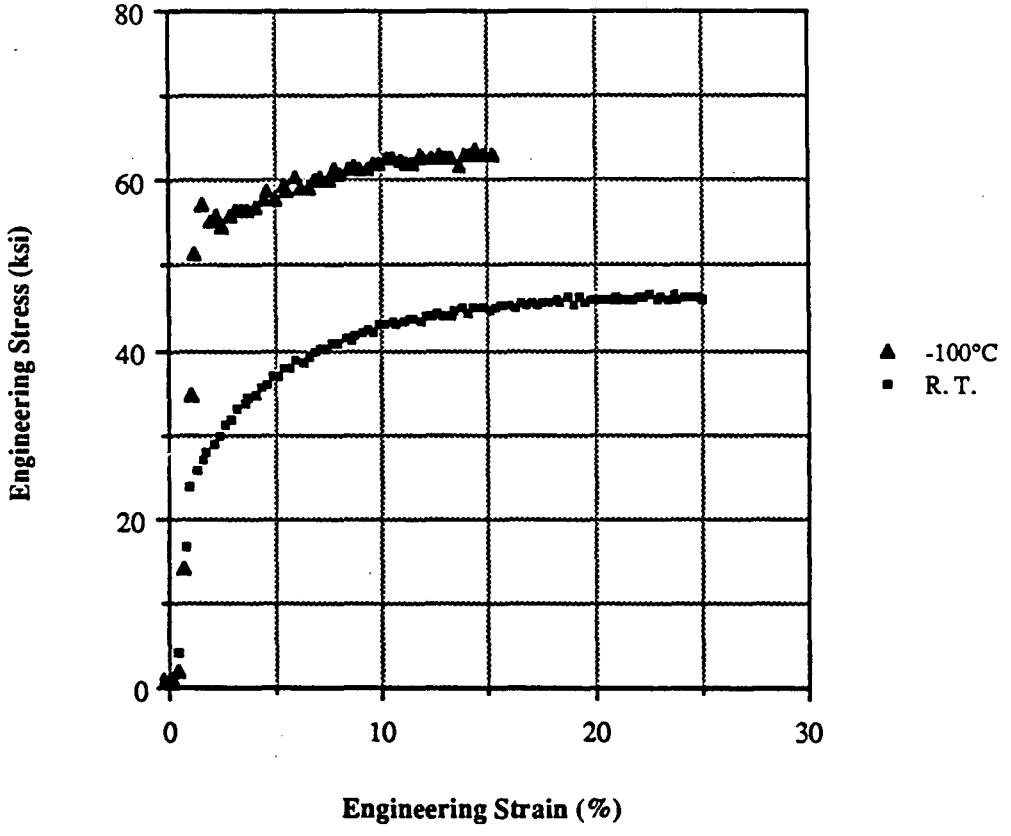

Figure 11. Tensile behavior at room temperature and -100°C (composite of Figures 5 and 6).

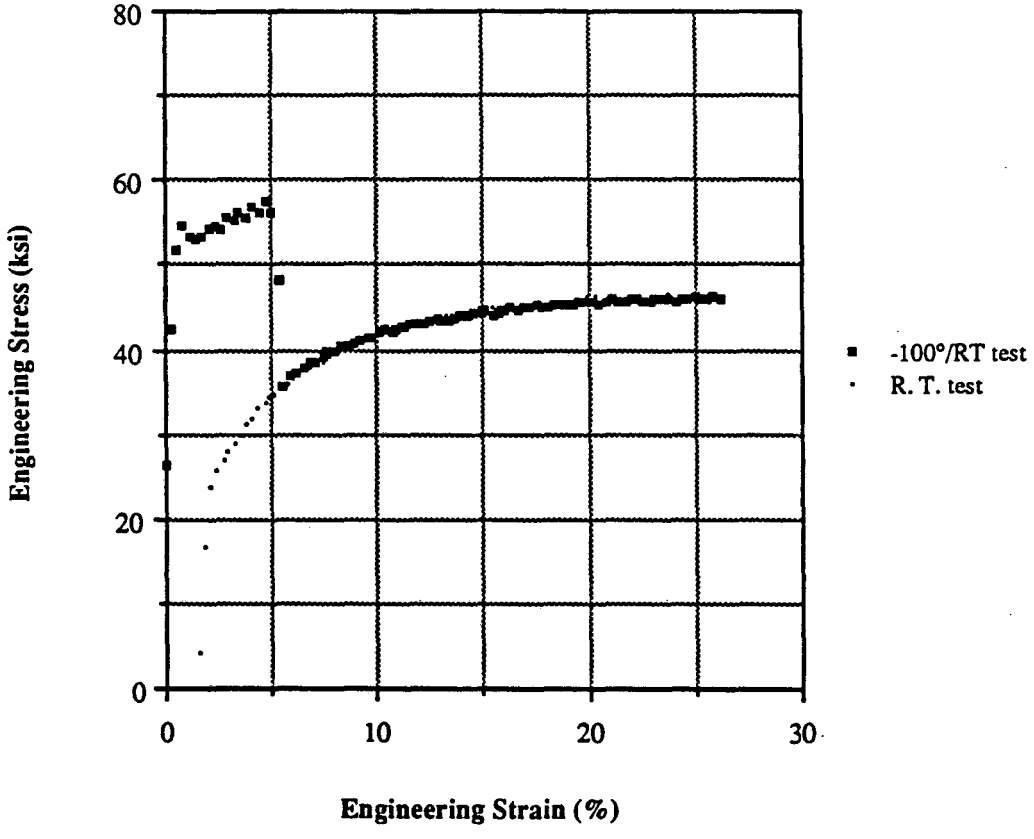

Figure 12. Comparison of room temperature tensile behavior (Figure 5), and tensile behavior of specimen deformed to 5% strain at -100°C, then to failure at room temperature (Figure 7).

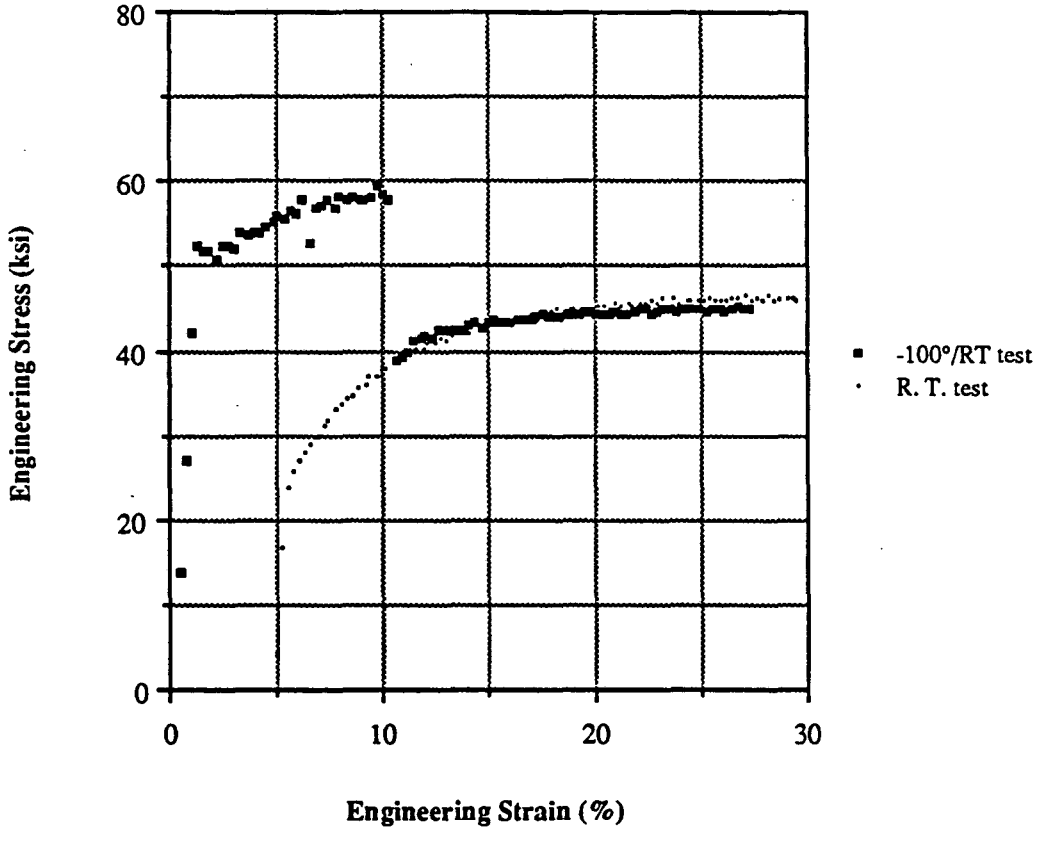

Figure 13. Comparison of room temperature tensile behavior (Figure 5), and tensile behavior of specimen deformed to 10% strain at -100°C, then to failure at room temperature (Figure 8).

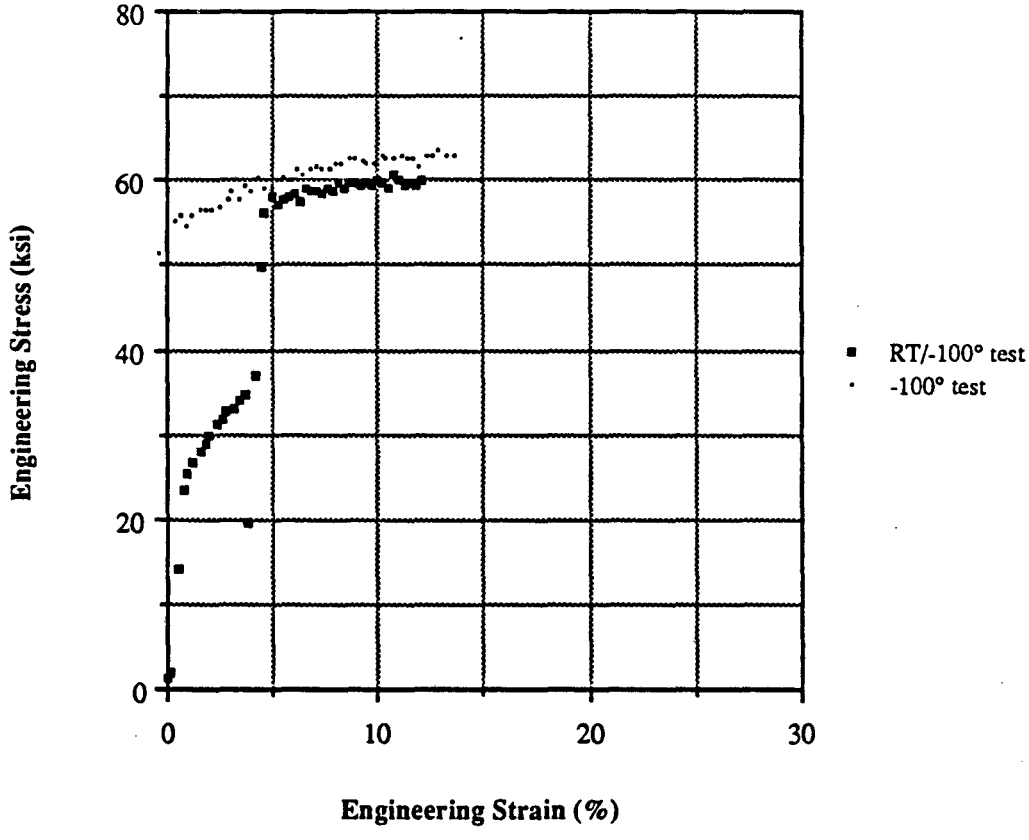

Figure 14. Comparison of -100°C tensile behavior (Figure 6), and tensile behavior of specimen deformed to RTFS-5% at room temperature, then to failure at -100°C (Figure 9).

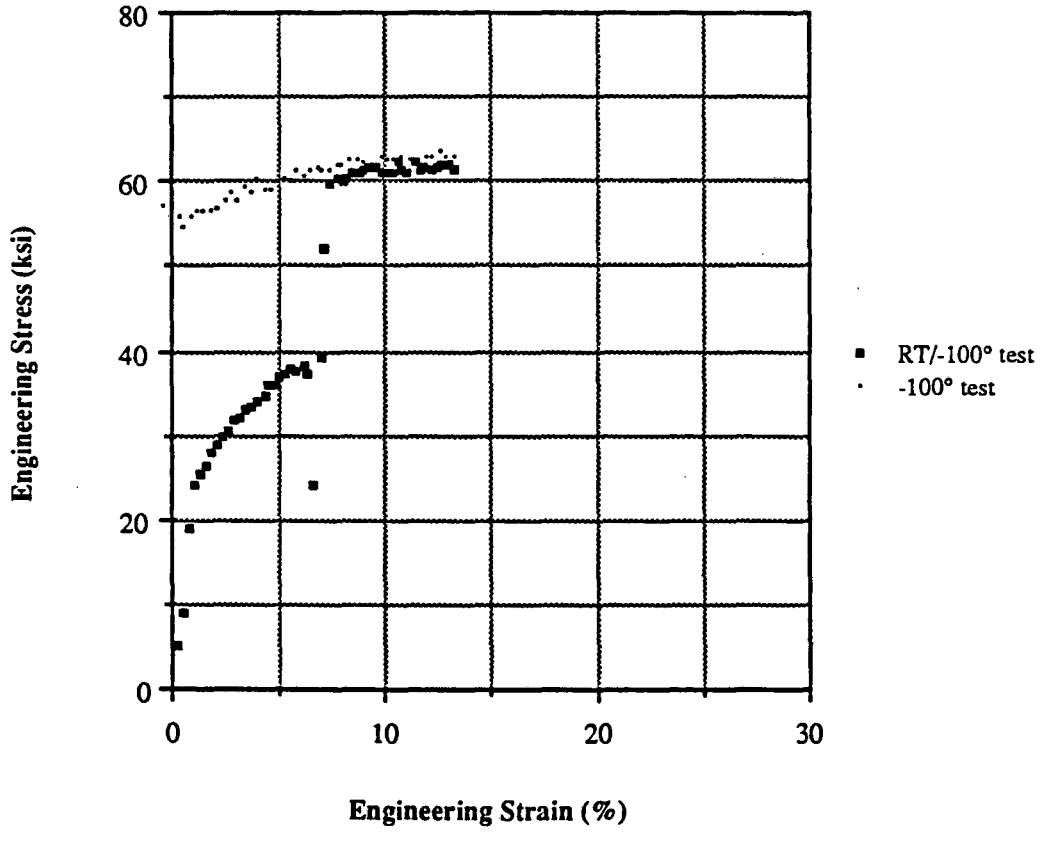

Figure 15. Comparison of -100°C tensile behavior (Figure 6), and tensile behavior of specimen deformed to RTFS-10% at room temperature, then to failure at -100°C (Figure 10).

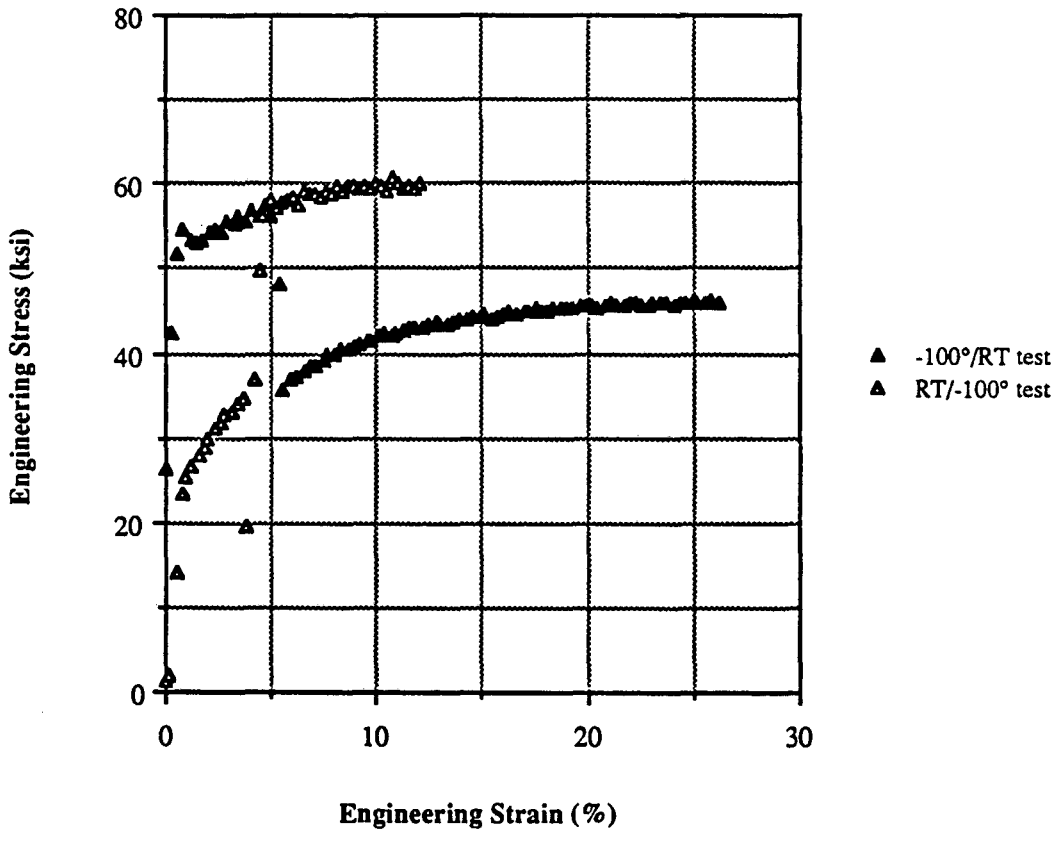

Figure 16. Comparison of tensile behavior from two tests in which the temperature was changed at RTFS-5% (composite of Figures 7 and 9).

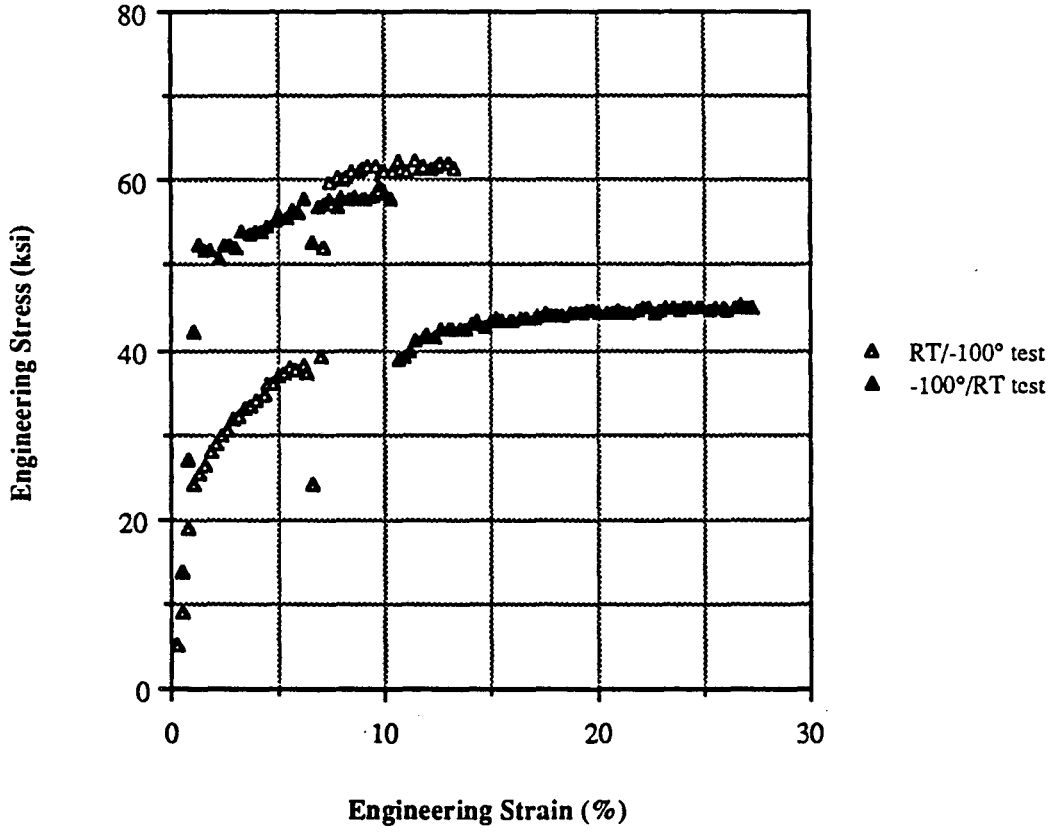

Figure 17. Comparison of tensile behavior from two tests in which the temperature was changed at RTFS-10% (composite of Figures 8 and 10).

Appendix 1: Data Management

The purpose of this appendix is to explain how the raw tensile data was processed to plottable form. The Fortran programs listed below were written for this function and executed using a Macintosh SE computer.

1. Input

The mechanical testing machine was connected to an IBM personal computer. Data from each test was stored by line, with five categories of data in each line: time, load, stroke, strain, and valve current (a measure of how well the actual test is following the computer-generated form). For processing this data was ported to a Macintosh Plus computer in the form of a MacTerminal file.

2. Strain-Stroke Calibration

Because the tests were generally performed to strains too large for the capacity of the strain gage, it was necessary to calculate the strain from the stroke. This calibration was accomplished by reading the strain and stroke from the MacTerminal file, plotting strain vs. stroke, and fitting a line to the data. The equation of the line was then used to convert stroke data to strain for plotting. Since the strain-stroke plots were linear, this method was found to give good results. This calibration was accomplished using a Fortran program written by David Chu. This program is listed on the following pages, entitled "Program 1: Strain-Stroke Calibration."

3. Calculation of Stress, Strain, and Strain Hardening Rate

Calculation of true stress and strain, engineering stress and strain, and strain hardening rate ($d\sigma / d\varepsilon$) was also done using a Fortran program written by David Chu. The functions of this program were to read the stroke and load data from the MacTerminal file, calculate both engineering and true stresses and strains, smooth the data, and calculate the strain hardening rate. This program is listed in the following pages (after Program 1), entitled "Program 2: Stress-Strain Calculations."

Program 1: Strain-Stroke Calibration

```
c program strk/strn
c
c This program was written by David Chu for the Morris Group
c       as requested by Sue Vincent. This program works with
c       the Emigh Testing Machine (ETM) which is at present
c       located in Building 8, Room 180.
c
c WARNING: This program was written specifically for the
c       fullfilment of requirements as specified by
c           Sue Vincent and hence may not work for anyone
c           else. If a separate version is required for
c           a different analysis, contact David Chu.
c
c
c Define variables
c
        character*10 label
        integer i, j, choice, nopnts, nosets, nrow, stop
        integer istrk, setsiz
        real temp
        real data, strain, stroke
        parameter (nrow=8000)
        dimension data(5)
        dimension istrk(nrow)
        dimension setsiz(nrow)
        dimension strain(nrow)
        dimension stroke(nrow)
c
c
c Prompt for information
c
        write (9) " Enter test file: "
        read(9,1100) label
c
c Read in the data points
c
        write (9) "Reading"
        open(3,file=label,status="old")
        do 10 i = 1,nrow
                if (mod(i,250) .lt. 1) then
                        write (9) "."
                end if
                read (3,*,end=20) (data(j),j=1,5)
                strain(i) = data(4)
                istrk(i) = ifix(data(3)*1000.0)
                nopnts = i
10      continue
        write (9,*) " "
        write (9,*) " DATA LIMIT REACHED : Proceed? (0=no,1=yes)"
        read (9,*) choice
        if (choice .ne. 1) then
```

```
                close(unit=3,status="keep")
                goto 90
        end if
20      close(unit=3,status="keep")
c
c Combine data according to strokes
c
        setsiz(1) = 1
        nosets = 1
        write (9,*) " "
        write (9) "Computing"
        do 40 i = 2,nopnts
                if (mod(i,250) .lt. 1) then
                        write (9) "."
                end if
                j=1
                stop = 0
30              continue
                if (stop .ne. 1) then
                        if (istrk(i) .eq. istrk(j)) then
                                strain(j) = strain(j) + strain(i)
                                setsiz(j) = setsiz(j) + 1
                                stop = 1
                        else if (j .ge. nosets) then
                                nosets = nosets + 1
                                istrk(nosets) = istrk(i)
                                strain(nosets) = strain(i)
                                setsiz(nosets) = 1
                                stop = 1
                        else
                                j = j + 1
                                stop = 0
                        end if
                goto 30
                end if
40      continue
        do 50 i = 1,nosets
                stroke(i) = float(istrk(i))/1000.0
                strain(i) = strain(i)/setsiz(i)
50      continue
c
c Place strains in numerical order
c
        write (9,*) " "
        write (9) "Ordering"
        stop = 0
60      continue
        if (stop .ne. 1) then
                stop = 1
                do 70 i = 2,nosets
                        if (stroke(i-1) .gt. stroke(i)) then
                                temp = stroke(i-1)
                                stroke(i-1) = stroke(i)
                                stroke(i) = temp
```

```
                                temp = strain(i-1)
                                strain(i-1) = strain(i)
                                strain(i) = temp
                                stop = 0
                        end if
70              continue
        goto 60
        end if
c
c Save routines
c
        write (9,*) " "
        write (9) "Saving"
        open(unit=4,file=".dat",status="new")
        write (4,1200) char(9)
        do 80 i = 1,nosets
                if (mod(i,250) .lt. 1) then
                        write (9) "."
                end if
        write (4,1300) stroke(i),char(9),strain(i)
80      continue
        close(unit=4,status="keep")
90      write (9) "   Okee Dokee...Bye for now. (<RETURN> to exit)"
        pause
c
c Format Statements
c
1100  format (a10)
1200    format ("    stroke",a1,"    strain")
1300    format (2(f10.3,a1))
        end
```

Program 2: Stress-Strain Calculations

```
c program sue
c
c This program was written by David Chu for the Morris Group
c       as requested by Sue Vincent. This program works with
c       the Emigh Mechanical Testing Machine which is at present
c       located in Building 8, Room 180.
c
c WARNING: This program was written specifically for the
c       fullfilment of requirements as specified by
c           Sue Vincent and hence may not work for anyone
c           else. If a separate version is required for
c           a different analysis, contact David Chu.
c
c
c Define variables
c
        character*10 label
        integer i, j, k, l, n, choice, endpnt, group
        integer lnyn, nopnts, nosets, nrow, ptf, pts
        integer sample, smooth, stop, strtpt
        integer istrn, setsiz
        real a, b, c, d, e
        real area, bint, calib, mslp, nwdata
        real temp, total
        real sumx, sumxx, sumxy, sumy, x, y
        real data, rate, strain, stress
        real egstrn, egstrs, trstrn, trstrs
        parameter (nrow=8000)
        dimension data(5)
        dimension egstrn(nrow)
        dimension egstrs(nrow)
        dimension istrn(nrow)
        dimension setsiz(nrow)
        dimension strain(nrow)
        dimension rate(nrow)
        dimension stress(nrow)
        dimension trstrn(nrow)
        dimension trstrs(nrow)
c
c
c Prompt for information
c
        write (9,1100) char(13)
        write (9,1100) char(13)
        write (9) " Enter test file: "
        read(9,1200) label
        write (9) " Enter cross-sectional area: "
        read(9,*) area
        write (9) " Enter calibration parameter: "
        read(9,*) calib
        write (9) " Enter group size (1,2,3,...,7): "
```

```
      read(9,*) group
      write (9) " Enter number of smoothing operations(0,1,2,...):  "
      read (9,*) smooth
      write (9) " Enter rate sampling size (3,5,7,...):  "
      read (9,*) sample
c
c Read in the data points
c
      write (9) "Reading"
      open(3,file=label,status="old")
      do 10 i = 1,nrow
            if (mod(i,100) .lt. 1) then
                  write (9) "."
            end if
            read (3,*,end=20) (data(j),j=1,5)
            stress(i) = data(2)/area
            istrn(i) = ifix(data(3)*calib*1000.0)
            nopnts = i
10    continue
      write (9,1100) char(13)
      write (9,*) " DATA LIMIT REACHED : Proceed? (0=no,1=yes)"
      read (9,*) choice
      if (choice .ne. 1) then
            close(unit=3,status="keep")
            goto 200
      end if
20    close(unit=3,status="keep")
c
c Combine data according to strains
c
      setsiz(1) = 1
      nosets = 1
      write (9,1100) char(13)
      write (9) "Computing"
      do 40 i = 2,nopnts
            if (mod(i,100) .lt. 1) then
                  write (9) "."
            end if
            j=1
            stop = 0
30          continue
            if (stop .ne. 1) then
                  if (istrn(i) .eq. istrn(j)) then
                        stress(j) = stress(j) + stress(i)
                        setsiz(j) = setsiz(j) + 1
                        stop = 1
                  else if (j .ge. nosets) then
                        nosets = nosets + 1
                        istrn(nosets) = istrn(i)
                        stress(nosets) = stress(i)
                        setsiz(nosets) = 1
                        stop = 1
                  else
                        j = j + 1
```

```
                        stop = 0
                    end if
                goto 30
                end if
40      continue
        do 50 i = 1,nosets
                strain(i) = float(istrn(i))/1000.0
                stress(i) = stress(i)/setsiz(i)
50      continue
c
c Place strains in numerical order
c
        write (9,1100) char(13)
        write (9) "Ordering"
        stop = 0
60      continue
        if (stop .ne. 1) then
                stop = 1
                do 70 i = 2,nosets
                    if (strain(i-1) .gt. strain(i)) then
                        temp = strain(i-1)
                        strain(i-1) = strain(i)
                        strain(i) = temp
                        temp = stress(i-1)
                        stress(i-1) = stress(i)
                        stress(i) = temp
                        stop = 0
                    end if
70              continue
        goto 60
        end if
c
c Group as requested
c
        nosets = ifix(nosets/group)
        do 90 i = 1,nosets
                j = i*group
                total = 0.0
                do 80 k = j-group+1,j
                    total = total + stress(k)
80              continue
                stress(i) = total/group
90      continue
        do 110 i = 1,nosets
                j = i*group
                total = 0.0
                do 100 k = j-group+1,j
                    total = total + strain(k)
100             continue
                strain(i) = (total/group)/100.0
110     continue
c
c Smooth data as requested
c
```

```
      do 130 i = 1,smooth
            write (9,1100) char(13)
            write (9) "Smoothing"
            temp = stress(1)
            do 120 j = 2,nosets-1
                  if (mod(j,100) .lt. 1) then
                        write (9) "."
                  end if
                  nwdata = temp + stress(j+1)
                  nwdata = nwdata + (2*stress(j))
                  temp = stress(j)
                  stress(j) = nwdata/4.0
120         continue
130   continue
c
c Checking values
c
      do 135 i = 1,10
      write (9,1300) strain(i),char(9),stress(i),char(9),rate(i)
135   continue
c
c Zero the plot as best as possible
c
      i = nint(5.0/group)
      call linreg (0,nrow,strain,stress,1,i,bint,mslp)
      do 140 j = 1,nosets
            strain(j) = strain(j) + (bint/mslp)
            egstrn(j) = strain(j)*100.0
            egstrs(j) = stress(j)
140   continue
c
c Checking values
c
      r = bint/mslp
      write (9,1300) r
      do 145 i = 1,10
      write (9,1300) strain(i),char(9),stress(i),char(9),rate(i)
145   continue
c
c Convert to true stress/strain
c
      do 150 i = 1,nosets
            strain(i) = log((strain(i))+1.0)
            stress(i) = stress(i)*exp(strain(i))
            trstrn(i) = strain(i)*100.0
            trstrs(i) = stress(i)
150   continue
c
c subtract elastic strain for strain hardening
c  rate calculation
c
      i = nint(5.0/group)
      call linreg(0,nrow,strain,stress,1,i,bint,mslp)
      do 160 i = 1,nosets
```

```
                strain(i) = strain(i) - (stress(i)/mslp)
160     continue
c
c calculate the strain hardening rate
c
        strtpt = 1
        do 170 i = 1,nosets
                if (strain(i) .le. 0.0) then
                        strtpt = i+1
                end if
                rate(i) = 0.0
170     continue
        write (9,1100) char(13)
        write (9) "Analyzing"
        endpnt = nosets - sample + 1
        do 180 i = strtpt,endpnt
                if (mod(i,100) .lt. 1) then
                        write (9) "."
                end if
                j = i
                k = i+sample-1
                l = i + ((sample-1)/2.0)
                stop = 0
                call linreg (1,nrow,strain,stress,j,k,bint,mslp)
                if ((bint .gt. 88.0) .or. (bint .lt. -80.0)) then
                        stop = 1
                end if
                if (mslp .lt. -35.0) then
                        stop = 1
                end if
                if (stop .eq. 1) then
                        rate(l) = 0.0
                else
                        rate(l) = (exp(bint))*mslp
                        rate(l) = rate(l)*(strain(l)**(mslp-1.0))
                end if
180     continue
c
c Save routines
c
        write (9,1100) char(13)
        write (9) "Saving"
        open(unit=4,file=".dat",status="new")
        write (4,1400) char(9),char(9),char(9)
        do 190 i = 1,nosets
                if (mod(i,100) .lt. 1) then
                        write (9) "."
                end if
                a = egstrn(i)
                b = egstrs(i)
                c = trstrn(i)
                d = trstrs(i)
                e = rate(i)
        write (4,1300) a,char(9),b,char(9),c,char(9),d,char(9),e
```

```
190     continue
        close(unit=4,status="keep")
        write (9,1100) char(13)
200     write (9) "   All done!...Bye for now.  <RETURN> to exit"
        pause
c
c Format Statements
c
1100    format (a1)
1200  format (a10)
1300    format (5(f10.3,a1))
1400    format ("eng strain",a1,"eng stress",a1,"tru strain",a1,"etc.")
        end


        subroutine linreg (lnyn,nrow,strain,stress,pts,ptf,bint,mslp)

        integer i, lnyn, n, nrow, pts, ptf
        real bint, mslp, sumx, sumy, sumxx, sumxy, x, y
        real strain, stress
        dimension strain(nrow)
        dimension stress(nrow)

        n = 0
        sumx = 0.0
        sumy = 0.0
        sumxx = 0.0
        sumxy = 0.0
        do 10 i = pts,ptf
                if (lnyn .eq. 1) then
                        x = log(strain(i))
                        if (stress(i) .le. 0.0) then
                                y = 0.0
                        else
                                y = log(stress(i))
                        end if
                else
                        x = strain(i)
                        y = stress(i)
                end if
                n = n + 1
                sumx = sumx + x
                sumy = sumy + y
                sumxx = sumxx + (x**2)
                sumxy = sumxy + (x*y)
10      continue
        mslp = ((n*sumxy)-(sumx*sumy))
        mslp = mslp/((n*sumxx)-(sumx**2))
        bint = ((sumy*sumxx)-(sumx*sumxy))
        bint = bint/((n*sumxx)-(sumx**2))
        return
        end
```

LAWRENCE BERKELEY LABORATORY
TECHNICAL INFORMATION DEPARTMENT
UNIVERSITY OF CALIFORNIA
BERKELEY, CALIFORNIA 94720